The landscape of DNA methylation associated with the transcriptomic network in laying hens and broilers gets insight into embryonic muscle development in chicken

Zihao Liu[£], Xiaoxu Shen[£], Shunshun Han[£], Yan Wang[£], Qing Zhu, Can Cui, Haorong He, Jing Zhao, Yuqi Chen, Yao Zhang, Lin Ye, Zhichao Zhang, Diyan Li, Xiaoling Zhao and Huadong Yin[#]

Farm Animal Genetic Resources Exploration and Innovation Key Laboratory of Sichuan Province, Sichuan Agricultural University, Chengdu, Sichuan 611130, PR China

[£] These authors contributed equally to this work.

[#] Corresponding author:

Huadong Yin, Farm Animal Genetic Resources Exploration and Innovation Key Laboratory of Sichuan Province, Sichuan Agricultural University, Chengdu, Sichuan 611130, PR China. E-mail: yinhuadong@sicau.edu.cn

Abstract

As DNA methylation is one of the key epigenetic mechanisms involved in embryonic development, elucidating its relationship with non-coding RNA and genes is essential for understanding early development of life. In this study, we performed single-base-resolution bisulfite sequencing together with RNA-seq to explore the genetic basis of embryonic muscle development in chicken. Comparison of methylome profiles between broilers and layers revealed that lower methylation in broilers might contribute to the muscle development. Differential methylated region analysis between two chicken lines showed that the majority of DMRs were hypo-DMRs for broilers. Differential methylated genes were significantly enriched in muscle development related terms at E13 and E19. Furthermore, by constructing the network of the lncRNA, we identified a lncRNA named MYH1-AS that potentially regulated muscle development. These findings depicted an integrative landscape of late period of embryonic myogenesis in chicken and gave rise to a comprehensive understanding of epigenetic and transcriptional regulation in the skeletal muscle development. In addition, our study provided a reliable epigenetic resource for further muscle studies.

Introduction

Epigenetics including DNA methylation, histone modification,

non-coding RNAs and chromatin remodeling fascinate researchers in recent year because of their essential roles in various biological processes[1,2]. The functions of epigenetics have been reported in many aspects such as in human diseases[3], oogenesis and spermatogenesis[4] as well as in adipose and muscle development[5-7]. DNA methylation is one of the epigenetic mechanisms that has been reported to exert considerable influence within regulation of the gene expression without changing the DNA methylation[8]. Its role in muscle development has been illustrated in human[9], pig[5,6], rabbit[10], bovine[11] and chicken as well[12].

Embryonic stage is crucial for mammal's muscle development as the number of muscle fiber keeps stable after birth. Therefore, it is interesting to study the embryonic muscle development from DNA methylation aspect. DNA methylation functioning in embryonic muscle development has been widely reported. For instance, ELVIRA CARRIO at el[13] built the methylome of myogenic stem cell and proved the importance of DNA methylation-mediated regulation of the cell-identity Myf5 super-enhancer during muscle-stem cell differentiation. Besides, lncRNAs were also proved to be important in regulation of muscle development for example, linc-MD1 interact with miR-133 and miR-135 to regulate the expression of transcription factors MAML1 and MEF2C that activate the muscle-specific gene expression[7]. Recently, the methylation and lncRNA regulatory relationship has drawn extensive attentions of researchers. A

database of methylation and lncRNA regulatory relationship has been built for human diseases studies[14]. In human, DNA methylation and lncRNA regulatory relationship were widely reported to be involve in tumorigenesis[15-17] whereas this regulatory relationship about muscle development is limited. The role of methylation in embryonic muscle development still remains unclear, although studies have been done in related field, such as Zhang at el[5] reported the regulatory relationship of lincRNA and DNA methylation functions in muscle development in pig. Yang at el[6] revealed that DNA methylation potentially affects gene expression in skeletal muscle to influence the propensity for obesity and body size.

The chicken is an ideal model for studying the embryogenesis and early muscle development because the accessibility of egg. Several genome-wide methylation studies have been reported in chicken. Basically, the relationship between DNA methylation level of promoter and expression level of genes were identified[18-20]. However, its role in chicken's embryonic muscle development has not been fully understood although global methylation landscape of muscle development was described in chicken using juvenile and later laying-period hens[12]. The ROSS 308 is one of the broilers bred and raised specifically for meat production whereas the Lohmann pink hen is a kind of layer bred and raised specifically for laying edible eggs. As they have

extremely different muscle accumulation and similar genetic background, they are good contrast model for muscle study. Here we used the whole genome bisulfite sequencing to produce the methylomes of 12 ROSS 308 and 12 Lohmann pink hen. In order to explore the effect of methylation and lncRNAs relationship on muscle development, we sequenced the whole transcriptome of these 24 samples by RNA-seq simultaneously for the multi-Omics integrative analyses.

Results

Overview of DNA Methylation

For genomic methylation data among 24 samples, the average sequence depth is about 30.3X. Approximately 3.4 billion reads were generated by the Illumina HiSeq in total and an average of 71.99% clean reads were mapped to the Gallus gallus genome (version 5.0) (Supplementary Table S1). The coverage analysis revealed that approximately 82% of the Gallus gallus genome were covered by reads at least one-fold, whereas nearly 78% of genome were covered more than 5-fold and 75% of genome were covered more than 10-fold (Supplementary Table S2). Those result indicated a reliable sequencing outcome.

The methylation level of each developmental stages was displayed in Fig 1a, revealing the layers and broilers have a similar global

methylation profile. The mCpGs in three different contexts showed similar proportion among 4 developmental stages (Fig 1b). Next, the methylation level distribution of mCpGs were analyzed at 4 developmental stages. Generally, mCpGs showed a high methylation level in mCG context whereas showed a low methylation level in mCHG and mCHH contexts (Fig 1c and Supplementary Fig 1a). Then we measured the methylation level of different regions of gene and compared those in different stages and populations. Interestingly, we found that broilers showed statistically lower methylation level at all stages in mCG context than layers (Fig 1d). Besides, CpG islands (CGIs) were identified and the numbers of CGIs at different regions were counted (Supplementary Fig 1b). we observed more CGIs located in promoter regions of gene in broilers than layers, which indicates methylation in CGIs may involve in muscle development as CGIs located at promoters regions are important for controlling gene expression[21].

Furthermore, the methylation level of lncRNAs assembled in RNA-seq of this experiment was also analyzed in similar way and compared with those of genes. Generally, broilers still showed lower methylation level in various types of lncRNA in mCG and mCHH contexts compared to laying hens whereas similar methylation level was observed among different types of lncRNA (Fig 2b and Supplementary Fig 2 c-d). Genes and lncRNAs had similar global methylation level and

both showed significant difference between two populations (Fig 2a and Supplementary Fig 2a-b). Those results suggest that faster muscle development of broilers may due to the lower methylation level in late embryonic stage compared with layer. Besides, the genomic distribution pattern of DNA methylation around genes and lncRNAs were analyzed. The upstream (2kb), first exon, first intron, internal exon, internal intron, last exon and downstream (2kb) of genes and lncRNAs across the genome were divided as different features and their methylation levels were measured through 20 bins, respectively. In general, the 5' upstream and 3'downstream regions were lower methylated than gene body regions. Besides, we also compared methylation level of features of gene with features of lncRNA (Fig 2c-d). It resulted that lncRNAs have relatively higher methylation level around TSS compared with genes ($P<0.001$). In addition, methylation levels of different types of repeat region were also analyzed across the genome. Beside the significant differences between two populations, short interspersed nuclear elements (SINE) particularly showed lower methylation level across 4 stages in mCG context (Fig 3 and Supplementary Fig 3).

Identification of differential methylation regions and genes.

To explore the potential causes of divergences in muscle development between broilers and layers, the differential methylation loci

(DMLs) were identified in DSS package. Then DMRs were identified for E10, E13, E16 and E19 respectively based on DMLs. The DMRs were subsequently annotated to the genome and the distribution of the DMRs in whole genome were analyzed (Fig 4a and Supplementary Table S4-S7). Generally, the majority of DMRs located in intronic regions whereas a small part of DMRs distributed in promoters of gene (Fig 4a). The proportion analysis revealed that broilers had more hypomethylated regions across the genome in four developmental stages, indicating that low methylation in muscle development-related genes may account for broiler's fast muscle development (Fig 4b).

Subsequently, the differential methylation genes (DMGs) were defined as genes overlapped with at least one DMR in its body region. The Gene Ontology (GO) enrichment analyses were performed to investigate potential biological functions of the DMGs. Generally, DMGs in four developmental stages were most significantly enriched in terms related to nervous system. However, many muscle-related terms were also found in the lists especially at DMGs of E13 and E19 such as muscle organ development (47 genes; Q-value < 0.001), myotube cell development (12 genes; Q-value < 0.005), positive regulation of muscle organ development (17genes; Q-value < 0.001), and muscle cell differentiation (51 genes; Q-value < 0.003) etc. (Fig 4c, Supplementary Table S8-S11). Because DMRs were not unanimous among different

developmental stages, we merged the genomic position of DMRs of 24 samples to form common DMRs and re-calculated the methylation level for each common DMR. The clustering analysis was performed using the common DMRs and displayed through heatmap. Different developmental stages were shown to cluster together which is indicative of the high quality of sampling and DMR calling in this experiment (Fig 5a). Moreover, the result of PCA was coincided with the clustering analysis (Fig 5b).

Integrative analyses of DNA methylation and transcriptome

To further explore whether methylation influences the gene and lncRNA expression in chicken, RNA-seq were used to measure the expression of genes and assembled novel lncRNAs. We identified 20656 lncRNAs in total (Fig 6a). Most of them are lincRNAs (63.6%) (Fig 6b). Heatmap of 24 samples and PCA suggested developmental stages accounted for most variances (Fig 6c). We divided genes and lncRNAs into 5 groups respectively based on their expression level (highest, medium high, medium low and lowest) using a quantile way. Then we measured their methylation level in different groups of genes and lncRNAs, respectively. Generally, broilers and layers were shown to have similar methylation levels and negative correlation was observed in genes in both populations as the highest expression level group showed lowest

196 methylation level around TSS whereas the lowest expression level group
197 showed the highest methylation level (Fig 6d, e). Interestingly, this
198 negative correlation trend between expression and methylation was
199 observed in downstream region of lncRNAs but not around TSS (Fig 6f,
200 g). Moreover, the lncRNAs are usually higher methylated around TSS
201 compared to genes (Fig 6d-g).

202 Next, the differential expression genes (DEGs) and lncRNA (DELs)
203 calling were performed for subsequent analysis. Meanwhile, the cis-target
204 and trans-target of lncRNAs were predicted, respectively. The DMRs
205 were assigned to lncRNAs generated from RNA-seq in this study
206 (Supplementary Table S12-S15) and the differential methylation lncRNA
207 (DM lncRNA) were defined as DEL overlapped with DMR. The result
208 showed that 55 DM lncRNAs were identified (13,16,11,15 in 4 stages,
209 respectively) (Supplementary Table S16). Subsequently, we looked for
210 DM lncRNA that was potential to regulate muscle development. In
211 particular, the expression of a lncRNA (we named it MYH1-AS, Fig 7a)
212 was highly correlated with methylation level of the DMR assigned to it
213 (Spearman, Cor=-0.7513, p<10^-4, Fig 7b). The expression of MYH1-AS
214 was detected to dramatically increase in broilers compared to laying hens
215 at E16 and E19 (Fig 8a). As the lncRNA was predicted by lncTar to
216 target several genes in MYH1 chicken-specific isoforms like MYH1A,
217 MYH1G, MYH1E etc., the expression correlations between the lncRNA

and its targets were calculated to search for its most likely target. Among its targets, MYH1E showed the highest correlation with MYH1-AS (Fig 7c), indicative of potential target of MYH1-AS. To further explore the role of MYH1-AS in muscle development, the gene-lncRNA networks were constructed based on their mRNA expression connectivity using WGCNA and the subnetwork of MYH1-AS was extracted from the whole network. It revealed that MYH1-AS had a high correlation with some muscle-related genes in this subnetwork (Fig 7d). Moreover, the relationship between connectivity and correlation was visualized in Fig 7f. Interestingly, genes highly negatively correlated with MYH1-AS did not show high connectivity with it. All genes showing high connectivity with MYH1-AS were also highly positively correlated with the lncRNA (Fig 7e-f). Then a total of 168 genes with top 50% both high connectivity and correlation with MYH1-AS were selected to perform GO enrichment analysis in order to confirm the role of MYH1-AS in muscle (Fig 7g and Supplementary S17). The result showed that the majority of terms enriched by those genes were muscle related.

Furthermore, the expressions of MYH1-AS produced by RNA-seq were verified through qPCR and it showed that similar trend was observed, indicating a reliable sequencing outcome (Fig 8 a, b). Subsequently, a siRNA was designed to perform MYH1-AS silencing assay. As shown in fig 8c, expression of MYH1-AS was significantly

reduced after transfecting, indicative of efficiency of siRNA used in this experiment (Fig 8c). Then the mRNA expression of muscle related genes (MyoD1, MyoG and MyH3) were measured at 48h after MYH1-AS silencing. It resulted in a reduced mRNA expression in silencing groups compared to control groups (Fig 8d-f). Besides, the microscope was used to monitor the morphological change in myotubes after silencing. We found that MYH1-AS silencing resulted in a reduced number of myotube (Fig 8g-h). Further western blot assay revealed that the protein expression of MyhC and MyoG was repressed in silencing groups (Fig 8i). Those results suggest that lncRNA MYH1-AS may function in muscle differentiation.

Discussion

The chicken provides a unique model to study embryology research of animal because of the accessibility of egg. As one of the most important energy sources for human diet, the muscle development of chicken is a significant commercial feature worthy for studies. In this study, the broilers and laying hens were used to explore the muscle development of chicken in late embryonic period as they are artificially selected for different commercial use thereby are divergent in muscle development. Because of the crucial role of methylation in embryogenesis[13], we performed whole genome bisulfite sequencing

(WGBS) and RNA-seq for to systematically explore the prenatal landscapes of chicken muscle development. Previous methylome studies have been done using prenatal chicken or born chicken muscle[12,22,23], however, those studies fails to display a comprehensive landscape of embryonic stages. We focused on more systematical study range from E10 to E19 between two chicken lines and aimed to elucidate the detain of embryonic muscle development.

The methylation level and proportion of different methylation contexts (mCG, mCHG, mCHH) of each developmental stage (Fig 1 a-d) indicated the layers and broilers have a similar global methylation profile. Additionally, the methylation level of different types of mCgG were measured (Fig 1 e-g). Those results are coincided with previous studies in chicken muscle[18]. The distribution proportion of mCpG in genome was different from the study of Zhang at el[23] as the mCpG in repeat region accounts for less genomic proportion in our study, probably because they used born chicken whereas the we performed the experiment on prenatal chicken. However, more studies were required to explore the detain.

We next comprehensively compared the methylation level of genes and lncRNAs among different developmental stages and chicken lines (Fig 2a). Generally, laying hens showed a significantly higher methylation level than broilers in mCG context in both genes and lncRNAs, which may be responsible for their divergences in muscle

development. Furthermore, different types of lncRNA (sense, intronic, antisense and lincRNA) were globally compared at methylation level and there were no significant differences among different types of lncRNAs, although layers and broilers still revealed significant variances (Fig 2b). Then genomic methylation around genes and lncRNAs were measured across the genome and the transcription start sites (TSS) were detected to be low methylated in genes (Fig 2c). The broilers and layers showed the similar trends around the transcription start site (TSS) which is coincident with the patterns of previous studies in chicken[12,18], as well as in bovine muscle tissue[11] and pig[24]. However, TSS of lncRNAs were usually higher methylated compare to genes (Fig 2c-d), which is able to explain why mRNA expression of lncRNAs are usually lower than genes ($P < 10^{-8}$) because methylation in promoter region usually affects gene expression[25]. In addition, the methylation level of different types of TEs (SINE, LINE, LTR, DNA and Satellite) were also measured in genome (Fig 3) and layers were found higher methylated than broilers in TEs regions. Transposable elements are usually inactivated in animals but TEs were reported to have a present-day function in early development of human and other mammals to provide cis-regulatory elements that co-ordinate the expression of groups of genes[26]. As epigenetic regulation is important for activity of TEs[27], the difference showed in the two chicken lines may also account for the divergence in development.

306 The clustering heatmap and principle component analysis (PCA)
307 were performed using common DMRs among 4 developmental stages.
308 The expected classifications were observed in both analyses and indicated
309 the reliable outcomes of sequencing and DMR calling (Fig 5a-b).
310 Moreover, we found that DMRs between two chicken lines mainly
311 distributed in intron regions and intergenic regions (Fig 4a), whose result
312 is coincide with previous study in chicken[12], indicative of its important
313 role in development regulation. However, as methylation in gene body
314 region affects gene expression in several sophisticated ways[21], further
315 studies on how methylation of the intron regions influences gene
316 expression are required to elucidate the complicated epigenetic
317 mechanism underlying development in chickens. Furthermore, the
318 proportion of hyper and hypo methylated regions were analyzed and the
319 majority of DMRs were detected to be hypomethylated regions in broilers,
320 indicating that low methylation may be responsible for fast muscle
321 development. This result was coincided with former result in this study
322 (Fig 4b, Fig 2a-b). Subsequently, genes with overlapped with DMR at
323 different times were regarded as DMGs and used for GO enrichment
324 analysis, respectively. We found that DMGs at E13 and E19 were
325 significantly enriched in muscle related terms, suggesting that
326 methylation play an important role in embryonic stage muscle
327 development. Additionally, DMGs among 4 stages were both

significantly enriched in nerve development related terms, which may relate to the impact of domestication and artificial breeding. Integrative analysis was conducted to study the association between methylation level and mRNA expression. We noticed that mRNA and methylation level around TSS were negative correlated in genes which was widely proved but not lncRNAs, indicating that DNA methylation regulates lncRNA expression in a more complex way.

To explore which lncRNA may potentially influence muscle development, the DM lncRNAs were identified and the correlation between DM lncRNA and DMR assigned to it were measured. In particular, we noticed that MYH1-AS showed high correlation with its target MYH1E and the DMR located in its intron region. Further WGCNA analysis revealed that some muscle related genes were highly correlated with MYH1-AS in its subnetwork (Fig 7d). For example, MYLK2, a muscle-specific gene, expresses skMLCK specifically in skeletal muscles[28,29]. ABLIM1 was reported to be related to muscle weakness and atrophy[30]. Increased PDK4 expression may be required for the stable modification of the regulatory characteristics of PDK observed in slow-twitch muscle in response to high-fat feeding[31] and some other genes in the network such as MyoZ1, MYPN, ZBTB16 etc. were also revealed to be muscle or meat quality related genes[32-35]. Therefore, it is reasonable that MYH1-AS functions in muscle development. Notably, as

we noticed that high correlation did not exactly mean high connectivity either (Fig 7e), we also performed GO enrichment analysis using 168 genes which had top 50% both high connectivity and correlation values with MYH1-AS in its network as input. It resulted in GO terms of which the majority were muscle related terms (Fig 7g), strongly indicative of the MYH1-AS functioning in muscle development. Therefore, it is reasonable to assume that MYH1-AS was regulated by DNA methylation and participated muscle development during embryonic stage. Subsequent silencing and western blot assay verified our analysis results, suggesting the reliability of our analysis and the role of MYH1-AS in muscle differentiation. However, how the lncRNA regulates muscle development requires more studies.

Our experiment revealed a comprehensive landscape of DNA methylome and transcriptome during embryonic developmental stage. Besides, we also found one lncRNA named MYH1-AS may potentially play a part in muscle development in chicken and provided evidence for this conclusion. Moreover, we provided a resource for further investigating the genetic regulation of methylation and gene expression in embryonic chicken. However, more studies are needed to elucidate the detailed mechanism how DNA methylation impacts lncRNA expression and how the lncRNA regulates myogenesis.

372 **Materials and Methods**

373 **Sample collection**

374 The fertilized eggs of Rose and WhiteLoghorn were incubated in the
375 same condition. The breast muscle and blood were collected at E10, E13,
376 E16, E19. After sex determination, only samples identified as male were
377 kept for next experiment. A total of 24 embryonic chicken were used in
378 the study to form eight groups: E10, E13, E16, E19 for Rose and
379 WhiteLoghorn, respectively. Each group included 3 individuals as
380 biological replicates.

381

382 **DNA and RNA extraction**

383 Genomic DNA was extracted using an animal genomic DNA kit
384 (Tiangen, China) following the manufacturer's instructions. The DNA
385 integrity and concentration were measured by agarose gel electrophoresis
386 and NanoDrop spectrophotometer, respectively. Total RNA was isolated
387 using TRIzol (TAKARA, Dalian, China) 110 reagent according to the
388 manufacturers' instruction. RNA was reverse 111 transcribed by
389 TAKARA PrimeScriptTM RT reagent kit (TAKARA) 112 according to
390 the manufacturers' instruction.

391

392 **Library construction and sequencing**

393 Bisulfite sequencing libraries were prepared using the TruSeq Nano

DNA LT kit (Illumina, San Diego, CA, USA). The genomic DNAs were then fragmented into 100–300 bp by sonication (Covaris, USA) and purified using a MiniElute PCR Purification Kit (QIAGEN, Silicon Valley Redwood City, CA, USA). The fragmented DNAs were end repaired and a single 'A' nucleotide was appended to the 3′ end of each fragment. After ligating the DNAs to the sequencing adapters, the genomic fragments were bisulfite converted via a Methylation-Gold kit (ZYMO, Murphy Ave. Irvine, CA, USA). The converted DNA fragments were PCR amplified and sequenced as paired-end reads using the Illunima HiSeq xten platform by the Biomarker Technologies company (Beijing, China).

Data alignment and process

The raw data in the FastQ format generated by the Illumina HiSeq were pre-processed by removing reads containing adapters, N (unknown bases) > 10%, and those which over 50% of the sequence exhibited low quality value (Qphred score ≤ 10). During the process, we also calculated the Q20, Q30, CG content for each sample data. The reads remained after this procedure were clean reads and used for subsequent analysis. The methylation data were aligned to reference genome Gallus gallus 5.0 by Bismark software[36]. Meanwhile, the number of aligned clean reads in unique position of reference genome were calculated as unique mapped

reads number. The proportion of the number of aligned reads in the total number of reads was calculated as the mapping rate. Subsequently, the methylation level of single base was then calculated by the ratio of the number of methylated reads to the sum of total reads covered the locus. Finally, we used a binominal distribution teat approach to determine whether a locus was regarded as methylated locus with the criteria: coverage depth > 4 and FDR<0.05[36].

The transcriptional libraries were sequenced on an Illumina HiSeq xten platform at the Biomarker Technologies Company (Beijing, China). The obtained transcriptome data were filtered by removing sequences containing adaptors, low-quality reads (Q-value < 20), and reads containing more than 10% of unknown nucleotides (N) and were aligned to reference genome Gallus gallus 5.0 by HISAT2[37] then the transcript assembly and FPKM calculation were performed using the StringTie[38]. Transcripts mapped to the coding genes of reference were used to subsequent differential expression gene calling.

LncRNA identification

In order to identify the potential lncRNA, the assembled transcripts generated from the StringTie were submitted to CPC[39], CNCI[40], CPAT[41] and pfam[42] software with defeat parameters to predict the potential lncRNAs. Only transcripts predicted as lncRNA shared among four tools

were regarded as candidate lncRNA. Then the cis-target gene of lncRNA were defined as neighbor gene in 100 kb genomic distance from the lncRNA and were identified using in-house script. The trans-target prediction of lncRNAs was performed by LncTar software[43].

DMLs and DMRs calling

The differential methylation locus (DMLs) and differential methylation regions (DMRs) between broilers and layers at each comparison were detected separately using Dispersion Shrinkage for Sequencing Data (DSS) package in R[44-47]. The differential methylation regions (DMRs) were then calculated in with default parameters. Subsequently, DMRs were annotated using ChIPseeker package in R[48].

Gene overlapped with at least one DMR is defined as differential methylation gene (DMG). Common DMRs among 4 developmental stages were identified by merging all positions of DMRs in 24 samples and re-calculating the methylation level for each merged DMR position with an average approach using mCpG data.

DEGs and DELs calling

The differential expression genes (DEGs) calling and the differential expression lncRNA (DEL) calling between two populations at each time point were performed separately using the DEseq[49]. The results were

filtering with the criteria: (1) fold change >2 (2) FDR<0.5. The transcripts satisfied both standards were regarded as DEGs or DELs.

Functional enrichment analysis and WGCNA analysis

Gene ontology enrichment analyses were conducted for DMGs at E10, E13, E16, E19 comparisons respectively to explore their potential roles in muscle development. These analyses were performed by clusterProfiler package implemented in R[50]. A hypergeometric test was applied to map DMGs to terms in the GO database to search for significantly enriched terms in DMGs compared to the genome background.

The WGCNA analysis was performed using WGCNA package implemented in R[51]. We used all the differential expression lncRNAs and all the genes as input. Then, variable coefficient was used to filter transcripts with low expression change. The variable coefficient was calculated as follow: $C_v = \sigma/\mu$. The σ is the standard deviation and μ represents the mean value of expression of input transcripts. Only transcripts with ranked top 30% high C_v value were used for WGCNA analysis. After the entire network was constructed, only genes with connectivity more than 0.15 were selected for subsequent subnetwork analysis.

Validation for RNA-seq by quantitative Real-time RCP(Q-PCR)

Total RNA was purified and reversely transcribed into cDNA using PrimerScriptR RT reagent Kit with gDNA Eraser (Takara Biotechnology (Dalian) Co., Ltd) following the specification. Quantities of mRNA were then measured with qRT-PCR using a CFX96TM real-time PCR detection system (Bio-Rad, USA). The qRT-PCR assays were then performed with a volume of 20 μL containing 10 μL SYBR Green Mixture, 7 μL deionized water, 1 μL template of cDNA, 1 μL of each primer and with following thermal conditions: 95 °C for 5 min, 45 cycles of 95 °C for 10 sec, 60 °C for 10 sec, 72 °C for 10 sec. Primer sequences used for qRT-PCR assays are displayed in Supplementary Table 17. β-actin gene was used as internal control. Each qPCR assay was carried out in triplicate. The relative gene expression was calculated by using the $2^{-\Delta\Delta Ct}$ method.

Cell cultures

Post-hatch chickens (7-day-old commercial generation Avian broiler chicks) were purchased from Wenjiang Charoen Pokphand Livestock & Poultry Co., Ltd. The pectoralis muscle was removed and used for preparation of primary myogenic cultures. About 5 g of muscle was finely minced and treated with 0.1% collagenase I (Sigma, MO, USA) followed by 0.25% trypsin (Hyclone, UT, USA) to release cells. Then, the cell

suspension was subjected to Percoll density centrifugation to separate myoblasts from contaminating myofibril debris and nonmyogenic cells. Cells were plated in 25 cm3 cell culture bottles with complete medium [DMEM/F12 (Invitrogen, Carlsbad, CA) +15% FBS (Gibco, NY, USA) +10% horse serum (Hyclone, UT, USA) +1% penicillin-streptomycin (Solarbio, Beijing, China) +3% chicken embryo extraction]. The cells cultured at 37 °C and 5% CO2 with saturating humidity, which were allowed to proliferate in growth medium for 2-4 d, and the medium was refresh every 24 h. To induce differentiation, satellite cells were grown to 80% confluence in growth medium, and the replaced with differentiation medium composed of DMEM, 2% horse serum and 1% penicillin-streptomycin, and the medium was refreshed every 24 h.

LncRNA silencing

Chicken satellite cells were cultivated in 6-well plates and transfected with siRNAs: 5'-GGAAGGGAGUAGGUGGUAATT-3' and 5'-UUACCACCUACUCCCUUCCTT -3'; Sangon Biotech, Shanghai, China) when grown to a density of approximate 70% in plates. In contrast, control cells were transfected with negative siRNA with same other condition. The transfection reagent was Lipofectamine 3000 (Invitrogen, Carlsbad, CA, USA). The knockdown efficiency was assessed by quantitative RT-PCR of lncRNA MYH1-AS.

Microscopy

Cellular morphology was evaluated in differentiated myotubes by phase-contrast microscopy without preliminary fixation. Pictures were produced using the Olympus IX73 inverted microscope (OLYMPUS, Tokyo, Japan) and the Hamamatsu C11440 digital camera (HAMAMATSU, Shizuoka, Japan).

Western blot assay

The cells were collected from the cultures, placed in the RIPA lysis buffer on ice (BestBio, Shanghai, China). The whole proteins were subjected to 10% sodium dodecyl sulfate polyacrylamide gel electrophoresis (SDS-PAGE) and then transferred to polyvinylidene fluoride membranes (PVDF; Millipore Corporation, Billerica, MA, USA). The PVDF membrane was incubated with 5% defatted milk powder at room temperature for 1 h, then incubation with the following specific primary antibodies at 4℃ overnight: anti-MyoG (Abcam), anti-MyHC (Abcam) and anti-β-Actin (Abcam). The secondary antibodies HRP-labeled rabbit IgG (Cell Signaling) were added at room temperature for 1h. Following each step, the membranes were washed five times with PBS-T for 3 min. The proteins were visualized by enhanced chemiluminescence (Amersham Pharmacia Biotech, Piscataway, NJ, USA) with a Kodak imager (Eastman Kodak, Rochester, NY, USA).

548 Quantification of protein blots was performed using the Quantity One
549 1-D software (version 4.4.0) (Bio-Rad, Hercules, CA, USA) on images
550 acquired from an EU-88 image scanner (GE Healthcare, King of Prussia,
551 PA, USA).

552

553

554

555

556

557

558

559

560

561

562

563

564

565

566

567

568

569

570 **Fig 1**. Genome-wide profiles of DNA methylation among different
571 sample groups. **(a)** Genomic methylation level in either layers or broilers
572 at E10, E13, E16, E19, respectively. Methylation level were range from 0
573 to 1. **(b-d)** Proportion of mCpG in different genomic features at different
574 developmental stages in mCG, mCHG and mCHH contexts, respectively.
575 **(e-g)** Methylation level of CpGs was equally divided into 10 intervals and
576 the percentage of each interval were measured using E10 as example.
577
578 **Fig 2**. Comparatively measurement of methylation level of genes
579 and lncRNA. **(a)** Comparison of methylation level of genes or lncRNAs
580 between layers and broilers in three different contexts. **(b)** Measurement
581 of methylation level of different types of lncRNAs. * P <0.05, ** P <0.01
582 for comparison between two chicken lines. The red star means the
583 methylation level of layers is significantly higher than broilers whereas
584 the green star represents an opposite result. **(c-d)** Genomic methylation
585 around genes and lncRNAs were measured across the genome,
586 respectively. Transcripts were separated into seven regions (upstream,
587 first exon, first intron, inner exon, inner intron, last exon and downstream)
588 and each region was equally divided into 20 bins for visualization.
589
590 **Fig 3**. Methylation level of different types of TEs using E19 as an
591 example. **(a)** Comparatively measurement of methylation of SINE, LINE,

592 LTR, DNA, Satellite regions between two chicken lines in mCG context.
593 **(b)** Methylation of different types of TEs for upstream, body and
594 downstream regions in three different contexts using 20 bins across the
595 whole genome.
596
597 **Fig 4**. Analyses of DMRs at 4 developmental stages. DMR calling
598 were performed in mCG, mCHG and mCHH, respectively. **(a)** Numbers
599 of DMRs in different genomic features (promoter, exon, intron, intergenic,
600 and UTR regions). **(b)** Relative proportion of hyper DMRs to hypo
601 DMRs in different CpG contexts. **(c)** The results of Gene Ontology (GO)
602 analysis for genes with overlapped with DMR. Only part of the terms was
603 selected for display. The red color means GO-BP terms, the blue color
604 means GO-CC terms whereas green color represents GO-MF terms. The
605 number in bracket means number of genes enriched in a specific term.
606
607 **Fig 5**. Heatmap clustering analysis and PCA analysis. **(a)** Heatmap
608 clustering using merged common DMRs among 24 samples (see
609 Materials and Methods). **(b)** The result of PCA analysis using common
610 DMRs among 24 samples. Only the first component and the second
611 component were visualized.
612
613 **Fig 6**. LncRNAs idenditication and correlation analysis between

614 methylome and transcriptome. **(a)** Number of different types of lncRNAs
615 in all developmental stages. **(b)** Venn diagram of lncRNAs identified
616 through different software. **(c)** Hierarchical cluster analysis of lncRNAs
617 using their expression level. Replicates were merged together in the
618 analysis. **(d-g)** The genes and lncRNAs were divided into five groups
619 based on their expression levels, respectively. Then the methylation level
620 around TSS and TES of each group were measured using 20 bins across
621 the whole genome for layers and broilers.
622
623 **Fig 7**. Comprehensive analysis of lncRNA MYH1-AS. **(a)**
624 visualization of the transcript of MYH1-AS and DMR overlapped it. **(b)**
625 Correlation between methylation of DMR and expression of MYHA-AS
626 using Spearman method. **(c)** Correlation between expression of
627 MYH1-AS and expression of its potential target MYH1E. **(d)** The whole
628 gene-lncRNA network and subnetwork including MYH1-AS extracted
629 from the entire network. (**e**) Relationship between correlation and
630 connectivity of gene and MYH1-AS. The red points represent genes with
631 both high connectivity and correlation with MYH1-A and were selected
632 for subsequent GO analysis. **(f)** Comparison of connectivity value
633 between genes selected (red points) and all genes with in the subnetwork
634 (background). * P <0.05, ** P <0.01 for comparison between selected
635 genes and background. **(g)** Results of GO analysis for genes selected.

Fig 8. **(a)** Expression level of MYH1-AS in layers and broilers at different developmental stages. **(b)** Verification of lncRNA MYH1-AS expression at four developmental stages by qPCR. **(c)** lncRNA Silencing efficiency. * P <0.05, ** P <0.01 for comparison between control and silenced group. **(d-f)** The mRNA expression of MyoD1, MyH3 and MyoG in control and MYH1-AS silenced groups, respectively. * P <0.05, ** P <0.01 for comparison between control and silenced group. **(g-h)** The morphological changes in myotubes after silencing. **(8i)** The protein expression of MyHC and MyoG comparison between control and silenced group, respectively.

658

659

660

661

662

663

664

665

666

667

668

669

670

671

672

673

674

675

676

677

678

679

References

1. Goldberg, A. D., Allis, C. D. and Bernstein, E. 2007, Epigenetics: a landscape takes shape. *Cell*, **128**, 635-638.
2. Guttman, M., Amit, I., Garber, M., et al. 2009, Chromatin signature reveals over a thousand highly conserved large non-coding RNAs in mammals. *Nature*, **458**, 223.
3. Feinberg, A. P. 2007, Phenotypic plasticity and the epigenetics of human disease. *Nature*, **447**, 433-440.
4. Sanford, J. P., Clark, H. J., Chapman, V. M. and Rossant, J. 1987, Differences in DNA methylation during oogenesis and spermatogenesis and their persistence during early embryogenesis in the mouse. *Genes & Development*, **1**, 1039-1046.
5. Zhou, Z. Y., Li, A., Wang, L. G., et al. 2015, DNA methylation signatures of long intergenic noncoding RNAs in porcine adipose and muscle tissues. *Scientific Reports*, **5**, 15435.
6. Yang, Y., Liang, G., Niu, G., et al. 2017, Comparative analysis of DNA methylome and transcriptome of skeletal muscle in lean-, obese-, and mini-type pigs. *Scientific Reports*, **7**.
7. Cesana, M., Cacchiarelli, D., Legnini, I., et al. 2011, A long noncoding RNA controls muscle differentiation by functioning as a competing endogenous RNA. *Cell*, **147**, 358-369.
8. Jaenisch, R. and Bird, A. 2003, Epigenetic regulation of gene expression: how the genome integrates intrinsic and environmental signals.
9. Miyata, K., Miyata, T., Nakabayashi, K., et al. 2015, DNA methylation analysis of human myoblasts during in vitro myogenic differentiation: de novo methylation of promoters of muscle-related genes and its involvement in transcriptional down-regulation. *Human Molecular Genetics*, **24**, 410-423.
10. Huszar, G. 1972, Developmental Changes of the Primary Structure and Histidine Methylation in Rabbit Skeletal Muscle Myosin. *Nature New Biology*, **240**, 260-264.
11. Huang, Y. Z., Sun, J. J., Zhang, L. Z., et al. 2014, Genome-wide DNA methylation profiles and their relationships with mRNA and the microRNA transcriptome in bovine muscle tissue (Bos taurine). *Scientific Reports*, **4**, 6546.
12. Zhang, M., Yan, F. B., Li, F., et al. 2017, Genome-wide DNA methylation profiles reveal novel candidate genes associated with meat quality at different age stages in hens. *Scientific Reports*, **7**, 45564.
13. Carriè´¸, E., Dé"†Ezvillanueva, A., Lois, S., et al. 2015, Deconstruction of DNA methylation patterns during myogenesis reveals specific epigenetic events in the establishment of the skeletal muscle lineage. *Stem Cells*, **33**, 2025-2036.
14. Zhi, H., Li, X., Wang, P., et al. 2017, Lnc2Meth: a manually curated database of regulatory relationships between long non-coding RNAs and DNA methylation associated with human disease. *Nucleic Acids Research*.
15. Zhang, C., Wang, X., Li, X., et al. 2017, The landscape of DNA methylation-mediated regulation of long non-coding RNAs in breast cancer. *Oncotarget*, **8**, 51134-51150.
16. Heilmann, K., Toth, R., Bossmann, C., Klimo, K., Plass, C. and Gerhauser, C. 2017, Genome-wide screen for differentially methylated long noncoding RNAs identifies Esrp2 and lncRNA Esrp2-as regulated by enhancer DNA methylation with prognostic relevance

for human breast cancer. *Oncogene*.

17. Wu, W., Bhagat, T. D., Yang, X., et al. 2013, Hypomethylation of noncoding DNA regions and overexpression of the long noncoding RNA, AFAP1-AS1, in Barrett's esophagus and esophageal adenocarcinoma. *Gastroenterology*, **144**, 956.
18. Li, J., Li, R., Wang, Y., et al. 2015, Genome-wide DNA methylome variation in two genetically distinct chicken lines using MethylC-seq. *Bmc Genomics*, **16**, 1-13.
19. Li, Q., Wang, Y., Hu, X., Zhao, Y. and Li, N. 2015, Genome-wide Mapping Reveals Conservation of Promoter DNA Methylation Following Chicken Domestication. *Sci Rep*, **5**, 8748.
20. Li, Q., Li, N., Hu, X., et al. 2011, Genome-wide mapping of DNA methylation in chicken. *Plos One*, **6**, e19428.
21. Jones, P. A. 2012, Functions of DNA methylation: islands, start sites, gene bodies and beyond. *Nature Reviews Genetics*, **13**, 484-492.
22. Li, S., Zhu, Y., Zhi, L., et al. 2016, DNA Methylation Variation Trends during the Embryonic Development of Chicken. *Plos One*, **11**, e0159230.
23. Hu, Y., Xu, H., Li, Z., et al. 2013, Comparison of the genome-wide DNA methylation profiles between fast-growing and slow-growing broilers. *Plos One*, **8**, e56411.
24. Wang, H., Wang, J., Ning, C., et al. 2017, Genome-wide DNA methylation and transcriptome analyses reveal genes involved in immune responses of pig peripheral blood mononuclear cells to poly I:C. *Scientific Reports*, **7**, 9709.
25. Lorincz, M. C., Dickerson, D. R., Schmitt, M. and Groudine, M. 2004, Intragenic DNA methylation alters chromatin structure and elongation efficiency in mammalian cells. *Nature Structural & Molecular Biology*, **11**, 1068-1075.
26. Garcia-Perez, J. L., Widmann, T. J. and Adams, I. R. 2016, The impact of transposable elements on mammalian development. *Development*, **143**, 4101-4114.
27. Waterland, R. A. and Jirtle, R. L. 2003, Transposable elements: targets for early nutritional effects on epigenetic gene regulation. *Molecular and cellular biology*, **23**, 5293-5300.
28. Kamm, K. E. and Stull, J. T. 2001, Dedicated myosin light chain kinases with diverse cellular functions. *Journal of Biological Chemistry*, **276**, 4527-4530.
29. Zhi, G., Ryder, J. W., Huang, J., et al. 2005, Myosin light chain kinase and myosin phosphorylation effect frequency-dependent potentiation of skeletal muscle contraction. *Proc Natl Acad Sci U S A*, **102**, 17519-17524.
30. Ohsawa, N., Koebis, M., Mitsuhashi, H., Nishino, I. and Ishiura, S. 2015, ABLIM1 splicing is abnormal in skeletal muscle of patients with DM 1 and regulated by MBNL, CELF and PTBP 1. *Genes to Cells*, **20**, 121-134.
31. Holness, M. J., Kraus, A., Harris, R. A. and Sugden, M. C. 2000, Targeted upregulation of pyruvate dehydrogenase kinase (PDK)-4 in slow-twitch skeletal muscle underlies the stable modification of the regulatory characteristics of PDK induced by high-fat feeding. *Diabetes*, **49**, 775-781.
32. Ying, F., Gu, H., Xiong, Y. and Zuo, B. 2017, Analysis of differentially expressed genes in gastrocnemius muscle between DGAT1 transgenic mice and wild-type mice. *BioMed research international*, **2017**.
33. Caremani, M., Yamamoto, D. L., Nigro, V., Lombardi, V., Bang, M. L. and Linari, M. 2014, The Role of Myopalladin in Skeletal Muscle. *Biophysical Journal*, **106**, 767a.

34. Shum, A. M., Mahendradatta, T., Taylor, R. J., et al. 2012, Disruption of MEF2C signaling and loss of sarcomeric and mitochondrial integrity in cancer-induced skeletal muscle wasting. *Aging (Albany NY)*, **4**, 133.
35. Luo, B., Ye, M., Xu, H., et al. 2018, Expression analysis, single-nucleotide polymorphisms of the Myoz1 gene and their association with carcase and meat quality traits in chickens. *Italian Journal of Animal Science*, 1-9.
36. Krueger, F. and Andrews, S. R. 2011, Bismark: a flexible aligner and methylation caller for Bisulfite-Seq applications. *Bioinformatics*, **27**, 1571-1572.
37. Kim, D., Langmead, B. and Salzberg, S. L. 2015, HISAT: a fast spliced aligner with low memory requirements. *Nature Methods*, **12**, 357.
38. Pertea, M., Pertea, G. M., Antonescu, C. M., Chang, T. C., Mendell, J. T. and Salzberg, S. L. 2015, StringTie enables improved reconstruction of a transcriptome from RNA-seq reads. *Nature Biotechnology*, **33**, 290-295.
39. Kong, L., Zhang, Y., Ye, Z. Q., et al. 2007, CPC: assess the protein-coding potential of transcripts using sequence features and support vector machine. *Nucleic Acids Research*, **35**, W345.
40. Sun, L., Luo, H., Bu, D., et al. 2013, Utilizing sequence intrinsic composition to classify protein-coding and long non-coding transcripts. *Nucleic Acids Research*, **41**, e166.
41. Wang, L., Park, H. J., Dasari, S., Wang, S., Kocher, J. P. and Wei, L. 2013, CPAT: Coding-Potential Assessment Tool using an alignment-free logistic regression model. *Nucleic Acids Research*, **41**, e74-e74.
42. Finn, R. D., Tate, J., Mistry, J., et al. 2011, A: The Pfam protein families database. *Nucleic Acids Research*, **32**, D138.
43. Li, J., Ma, W., Zeng, P., et al. 2015, LncTar: a tool for predicting the RNA targets of long noncoding RNAs. *Briefings in Bioinformatics*, **16**, 806.
44. Wu, H., Wang, C. and Wu, Z. 2012, A new shrinkage estimator for dispersion improves differential expression detection in RNA-seq data. *Biostatistics*, **14**, 232-243.
45. Feng, H., Conneely, K. N. and Wu, H. 2014, A Bayesian hierarchical model to detect differentially methylated loci from single nucleotide resolution sequencing data. *Nucleic acids research*, **42**, e69-e69.
46. Wu, H., Xu, T., Feng, H., et al. 2015, Detection of differentially methylated regions from whole-genome bisulfite sequencing data without replicates. *Nucleic acids research*, **43**, e141-e141.
47. Park, Y. and Wu, H. 2016, Differential methylation analysis for BS-seq data under general experimental design. *Bioinformatics*, **32**, 1446-1453.
48. Yu, G., Wang, L. G. and He, Q. Y. 2015, ChIPseeker: an R/Bioconductor package for ChIP peak annotation, comparison and visualization. *Bioinformatics*, **31**, 2382-2383.
49. Anders, S., Mccarthy, D. J., Chen, Y., et al. 2013, Count-based differential expression analysis of RNA sequencing data using R and Bioconductor. *Nature Protocols*, **8**, 1765.
50. Yu, G., Wang, L.-G., Han, Y. and He, Q.-Y. 2012, clusterProfiler: an R package for comparing biological themes among gene clusters. *Omics: a journal of integrative biology*, **16**, 284-287.
51. Langfelder, P. and Horvath, S. 2008, WGCNA: an R package for weighted correlation network analysis. *BMC bioinformatics*, **9**, 559.

811

Fig 1a

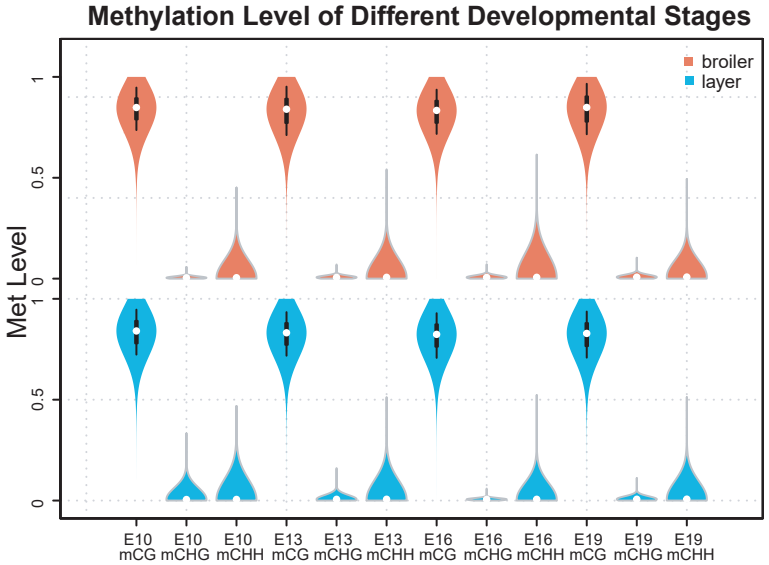

Fig 1b

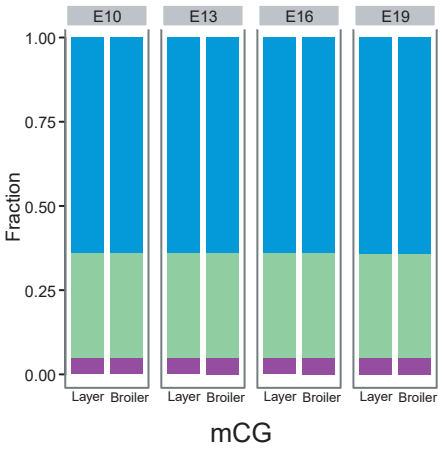

Fig 1c

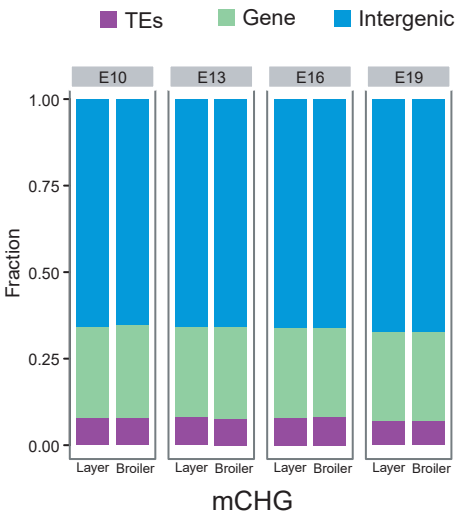

Fig 1d

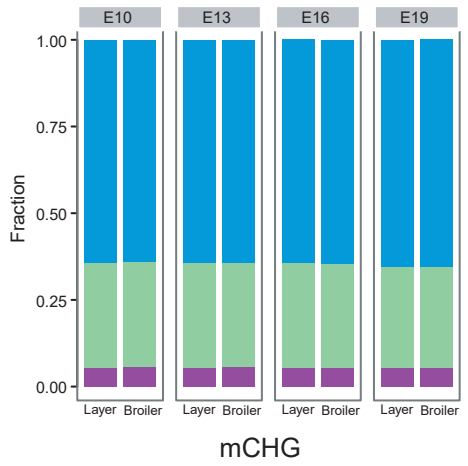

Fig 1e

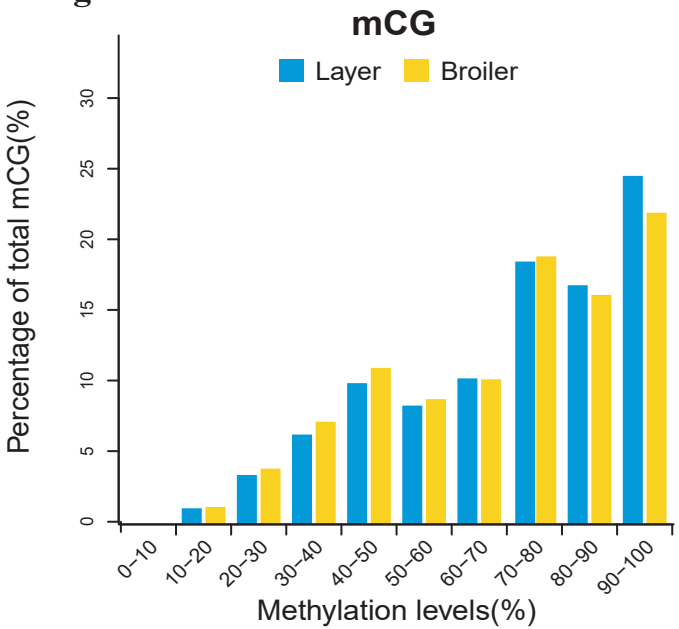

Fig 1f

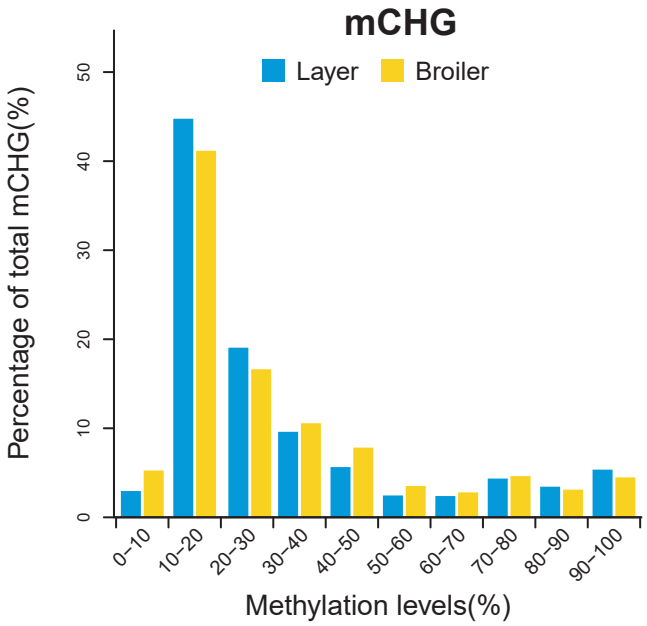

Fig 1g

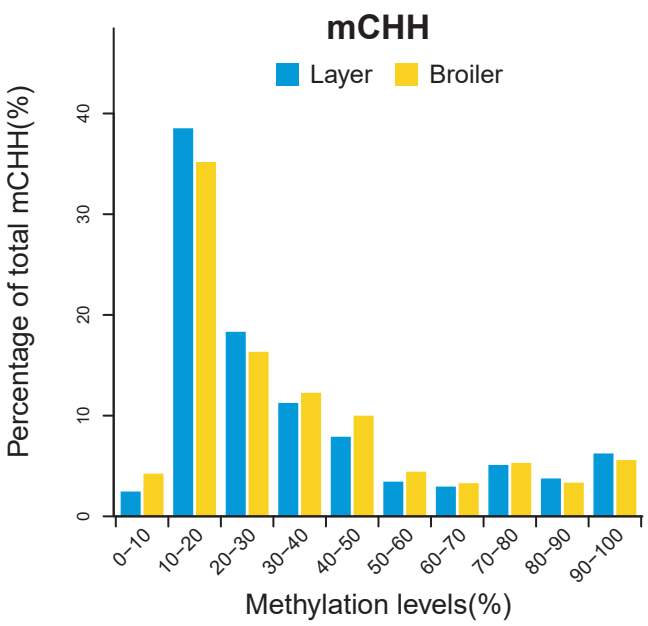

Fig 2a

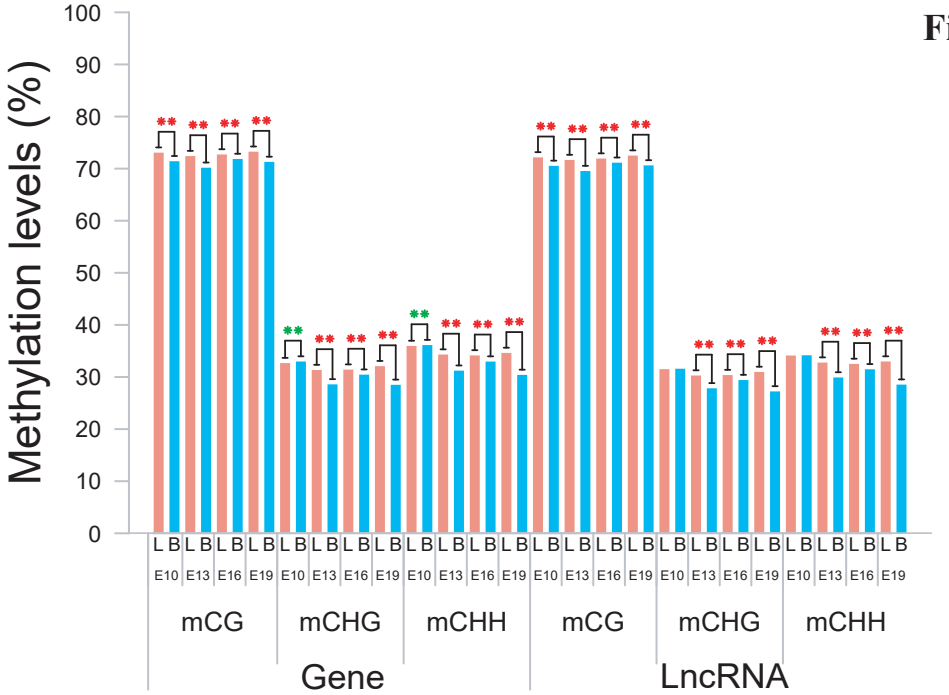

Fig 2b

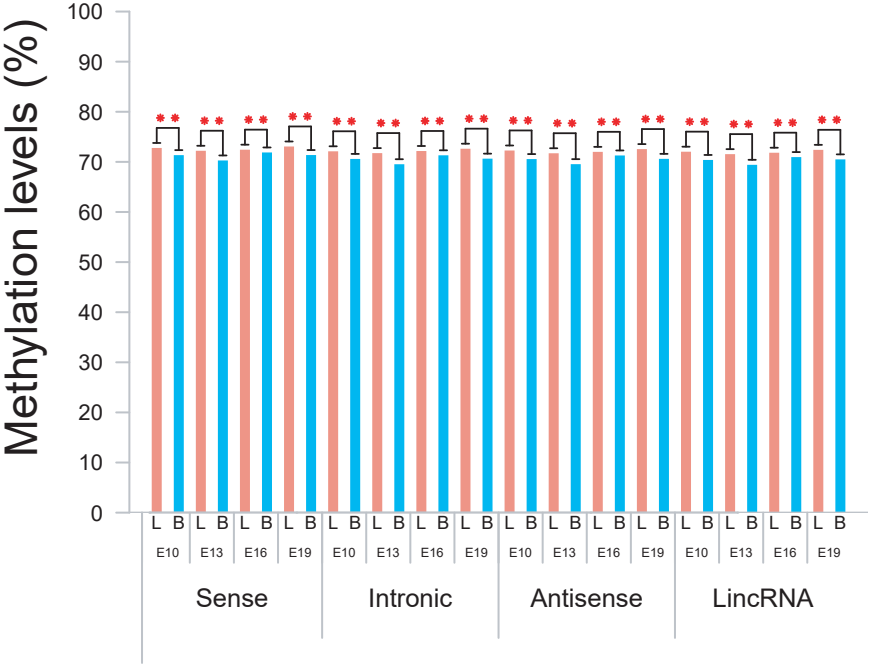

Fig 2c

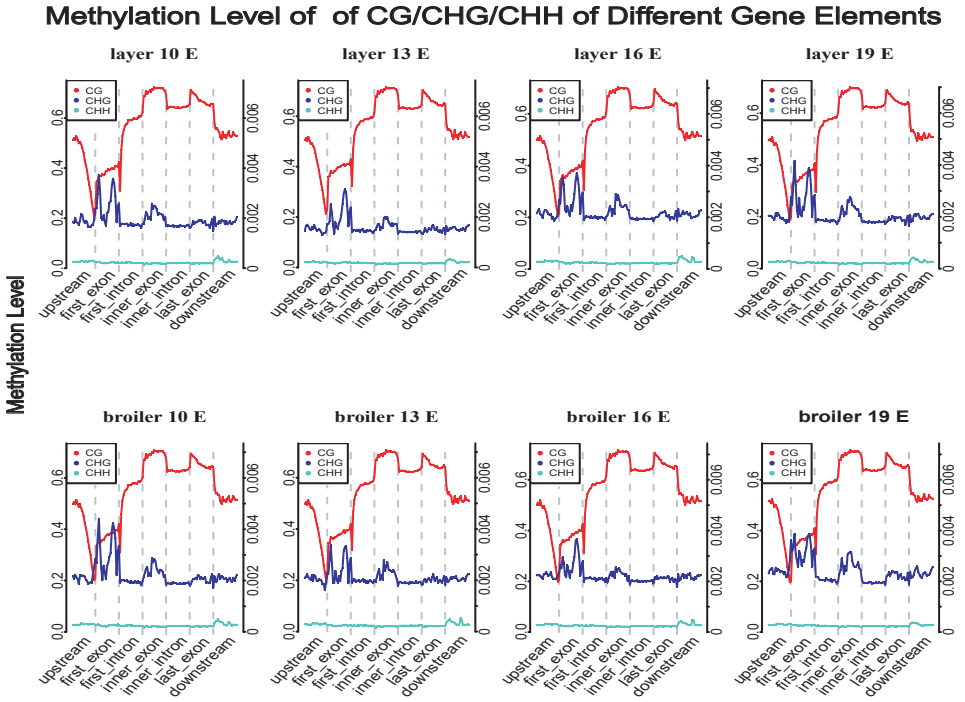

Fig 2d

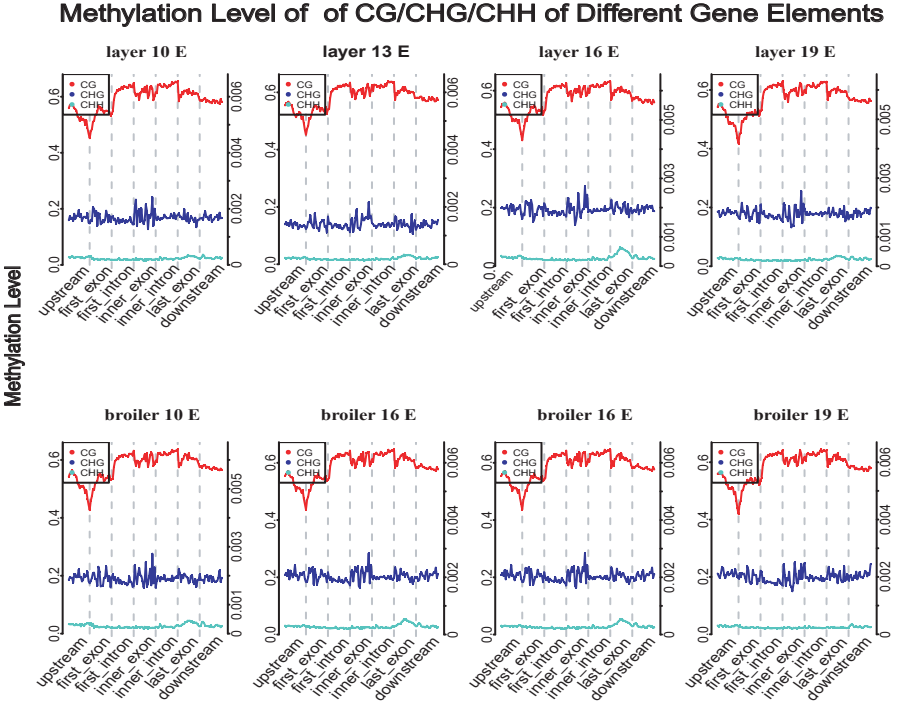

Fig 3a

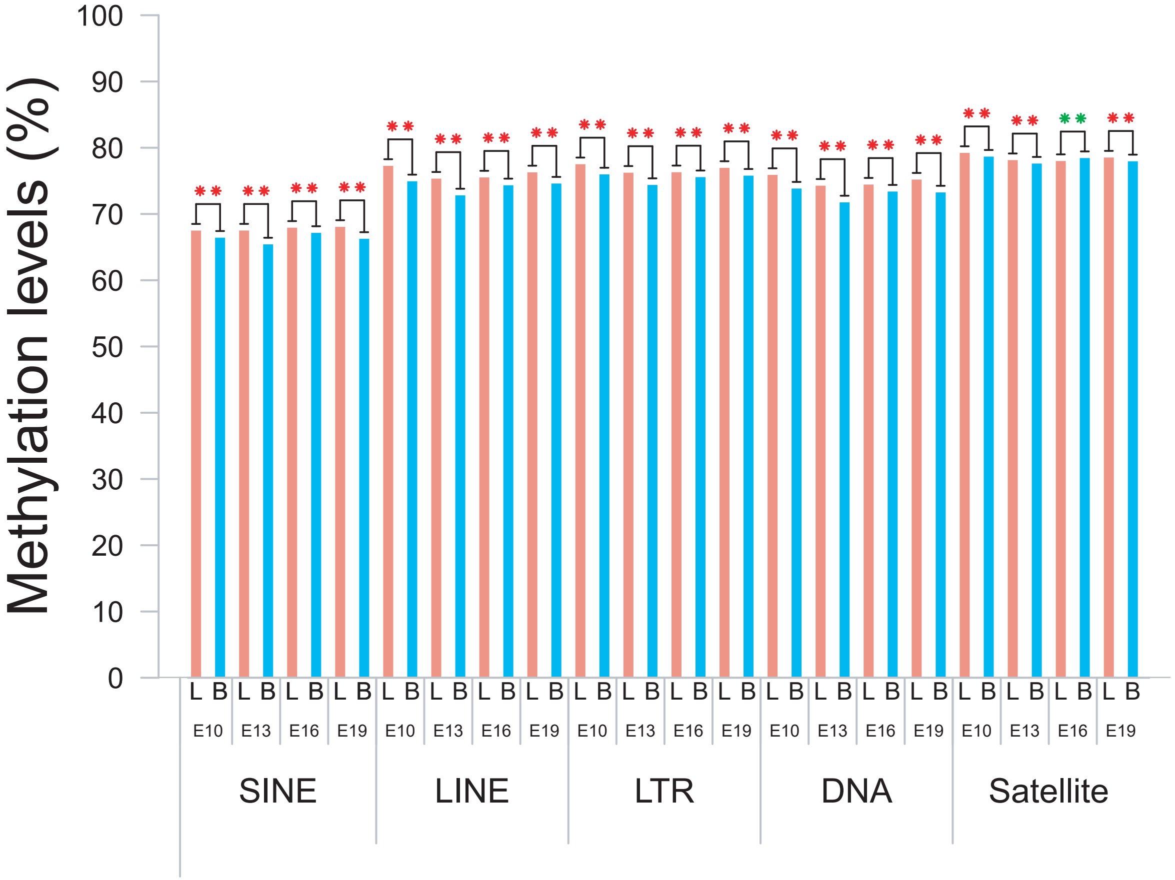
Methylation levels (%)
100
90
80
70
60
50
40
30
20
10
0
L B L B L B L B L B L B L B L B L B L B L B L B L B L B L B L B L B L B L B L B
E10 E13 E16 E19 E10 E13 E16 E19 E10 E13 E16 E19 E10 E13 E16 E19 E10 E13 E16 E19
SINE
LINE
LTR
DNA
Satellite

Fig 3b

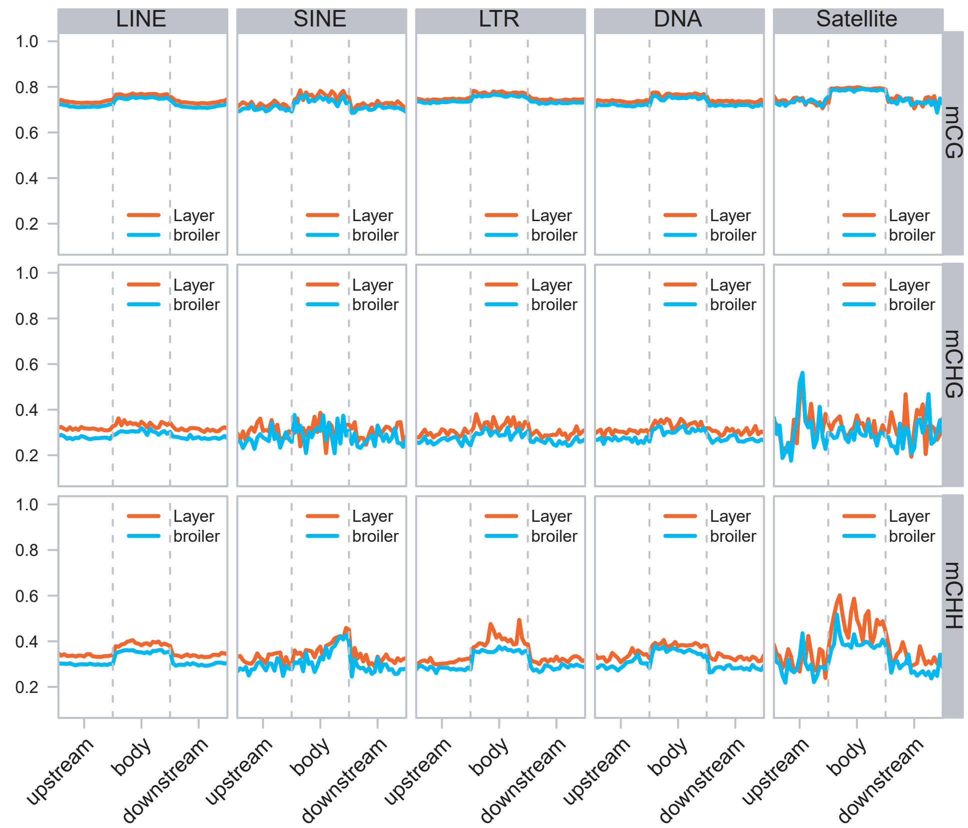
LINE
SINE
LTR
DNA
Satellite
mCG
mCHG
mCHH
Layer
broiler
1.0
0.8
0.6
0.4
0.2
upstream
body
downstream

Fig 4a

Fig 4b

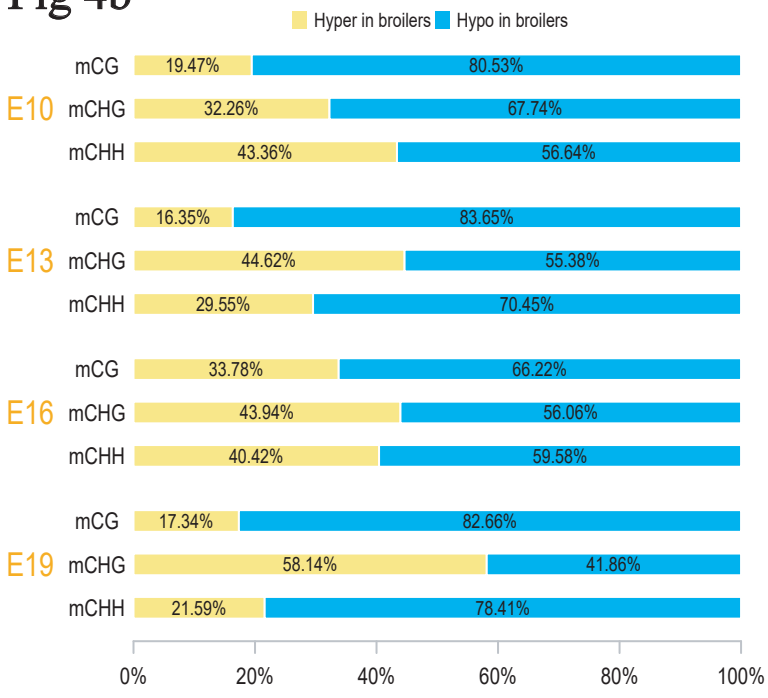

Fig 4c

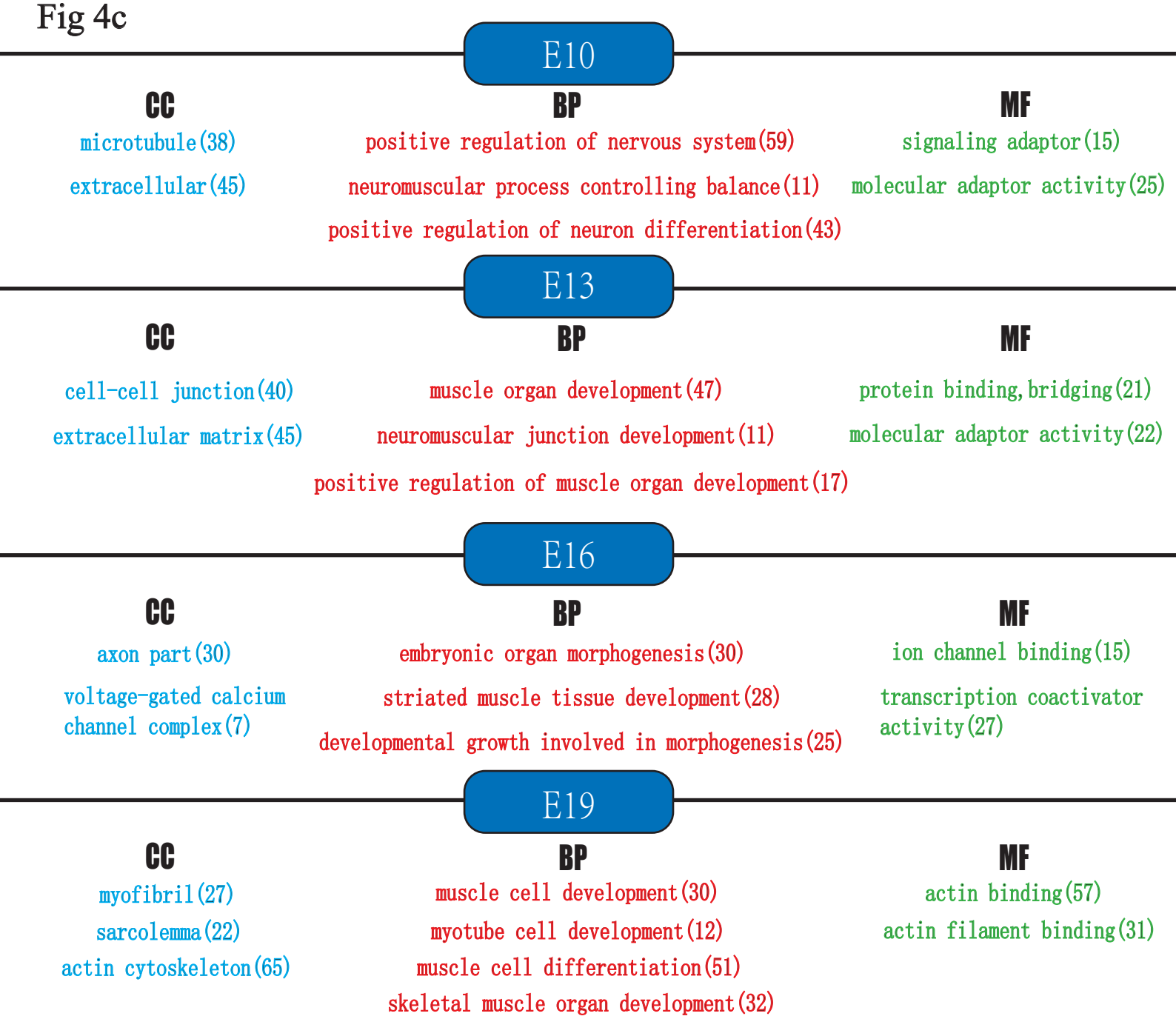

Fig 5a

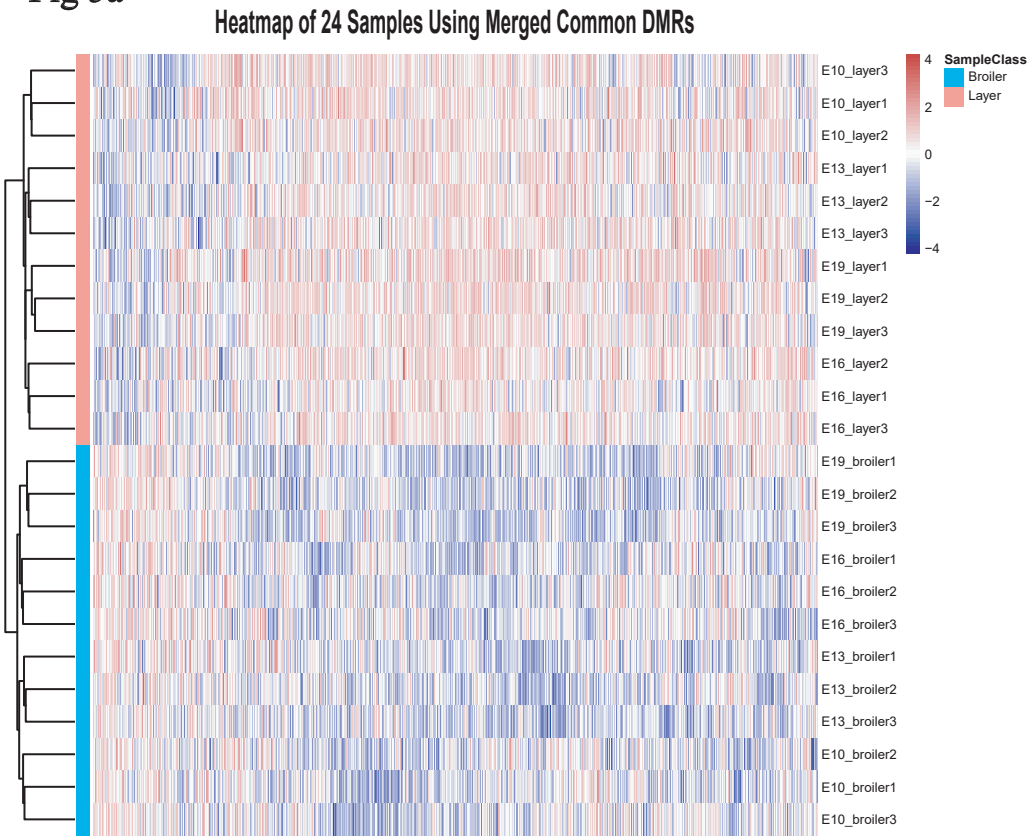
Heatmap of 24 Samples Using Merged Common DMRs
SampleClass
Broiler
Layer
4
2
0
−2
−4
E10_layer3
E10_layer1
E10_layer2
E13_layer1
E13_layer2
E13_layer3
E19_layer1
E19_layer2
E19_layer3
E16_layer2
E16_layer1
E16_layer3
E19_broiler1
E19_broiler2
E19_broiler3
E16_broiler1
E16_broiler2
E16_broiler3
E13_broiler1
E13_broiler2
E13_broiler3
E10_broiler2
E10_broiler1
E10_broiler3

Fig 5b

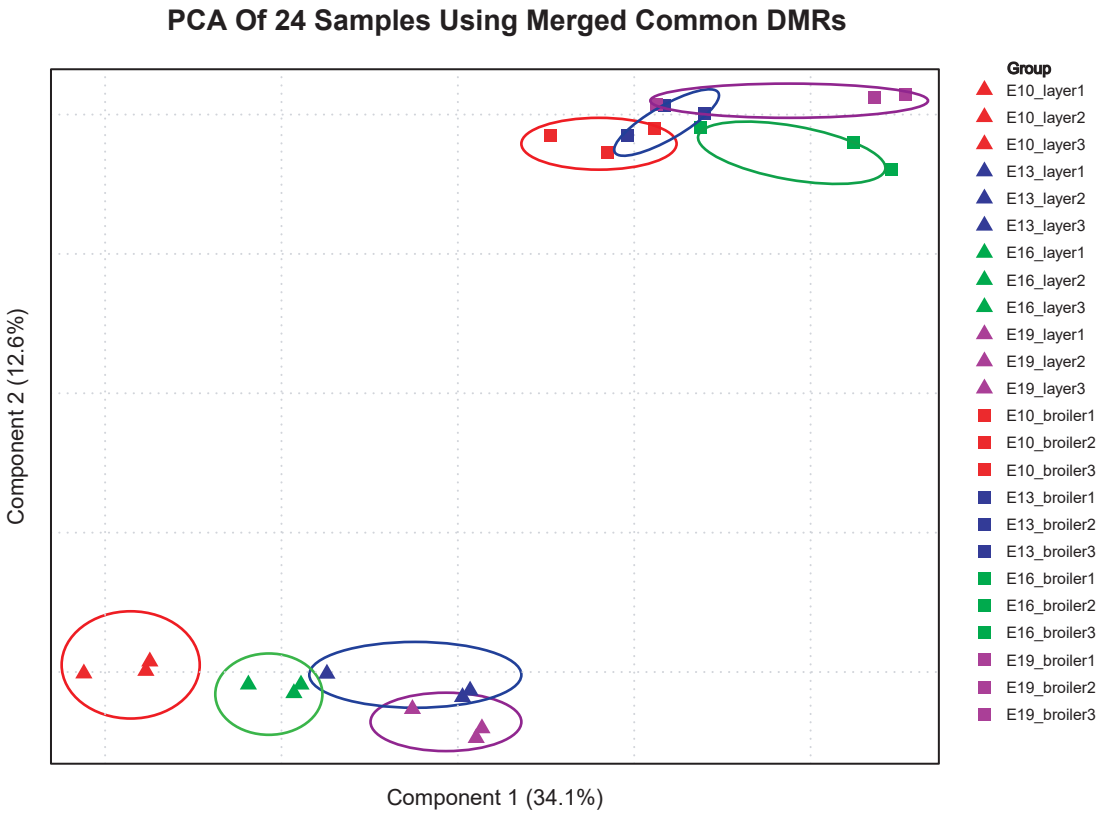
PCA Of 24 Samples Using Merged Common DMRs
Component 2 (12.6%)
Component 1 (34.1%)
Group
E10_layer1
E10_layer2
E10_layer3
E13_layer1
E13_layer2
E13_layer3
E16_layer1
E16_layer2
E16_layer3
E19_layer1
E19_layer2
E19_layer3
E10_broiler1
E10_broiler2
E10_broiler3
E13_broiler1
E13_broiler2
E13_broiler3
E16_broiler1
E16_broiler2
E16_broiler3
E19_broiler1
E19_broiler2
E19_broiler3

Fig 6a

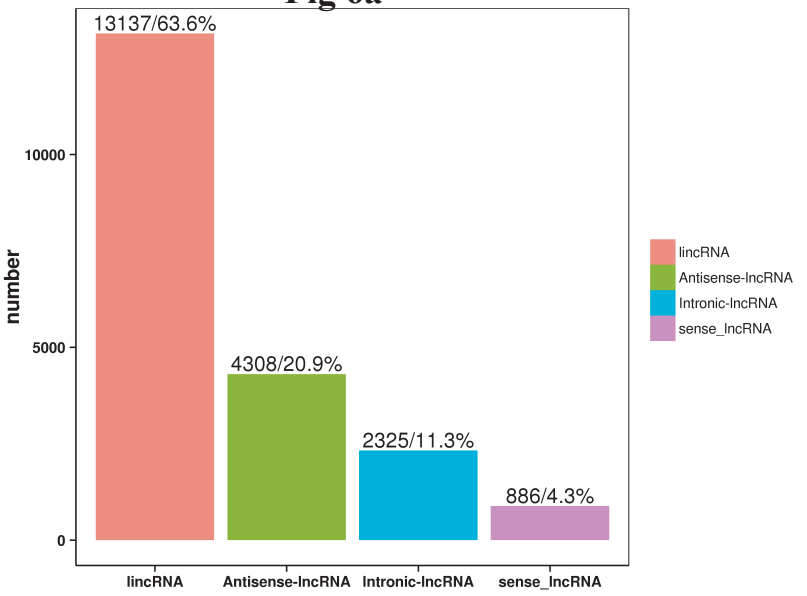

Fig 6b

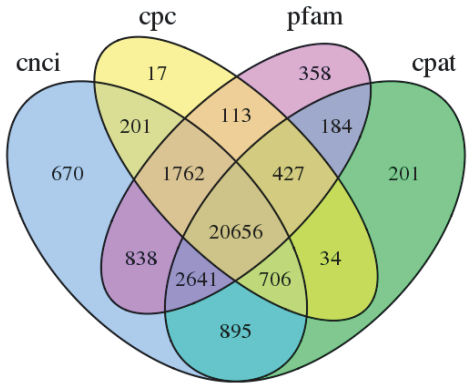

Fig 6c

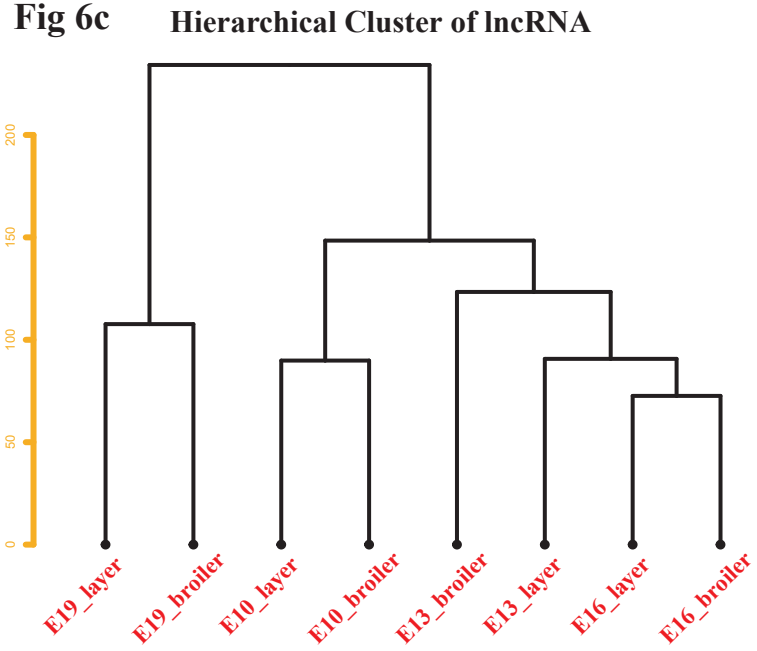

Fig 6d

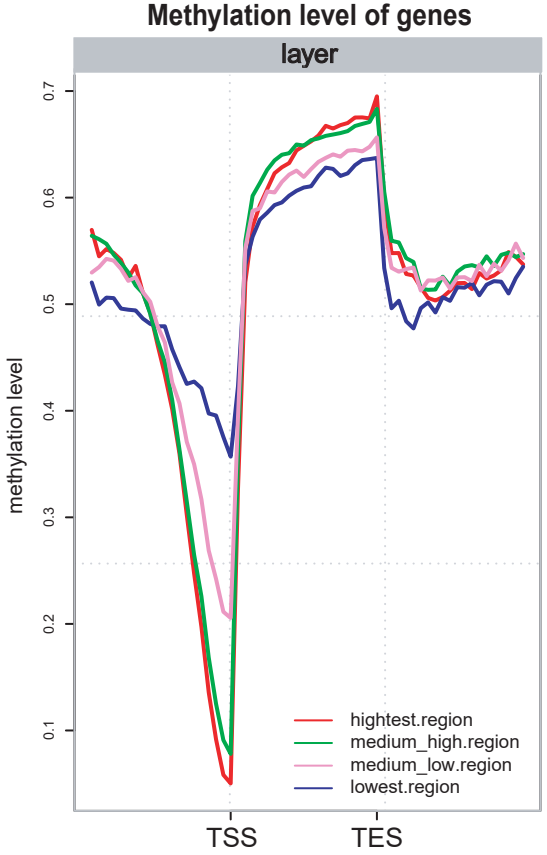

Fig 6e

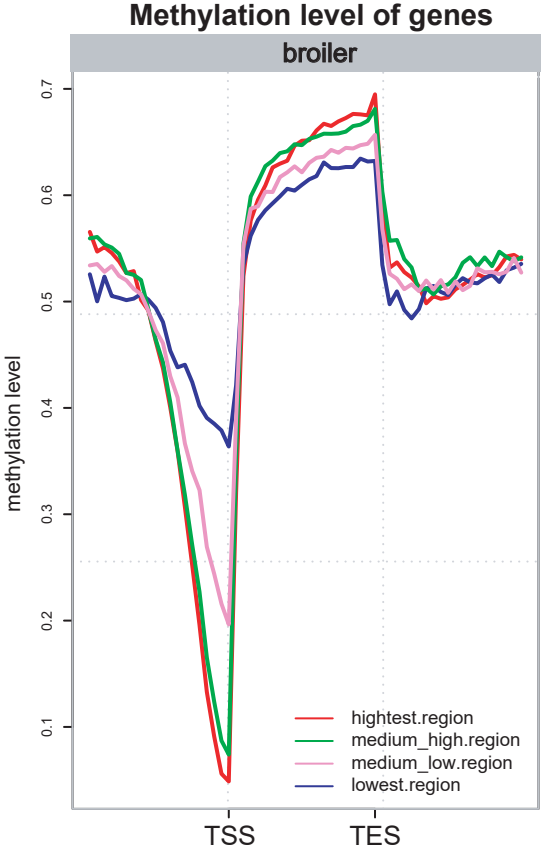

Fig 6f

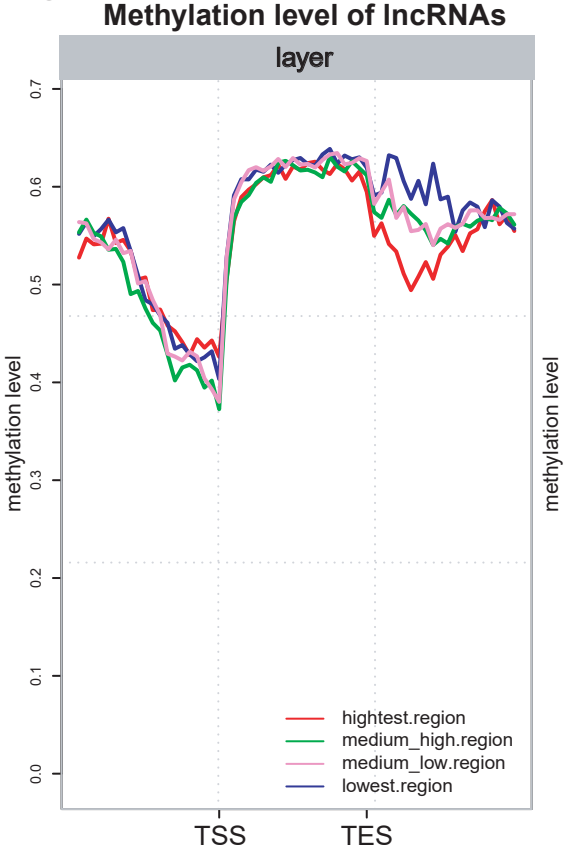

Fig 6g

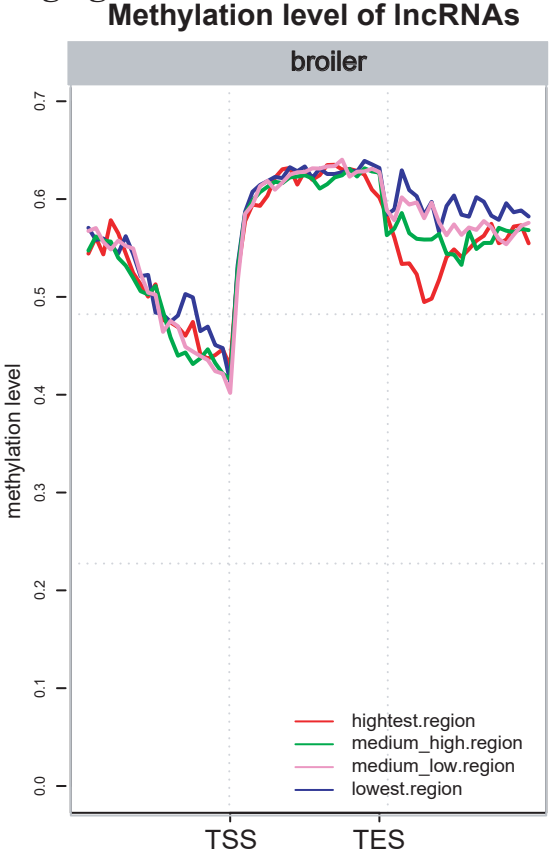

Fig 7a

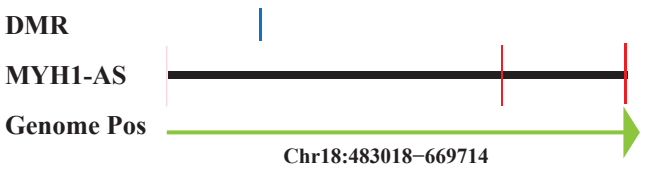

Fig 7b

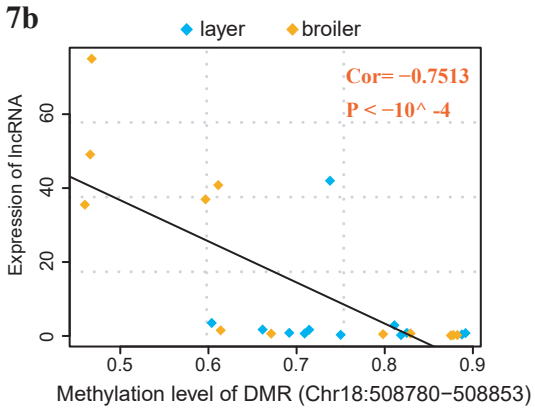

Fig 7c

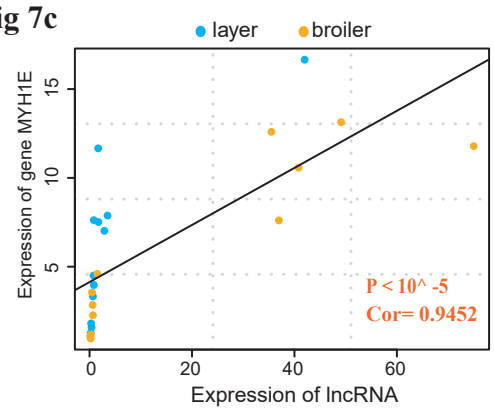

Fig 7d

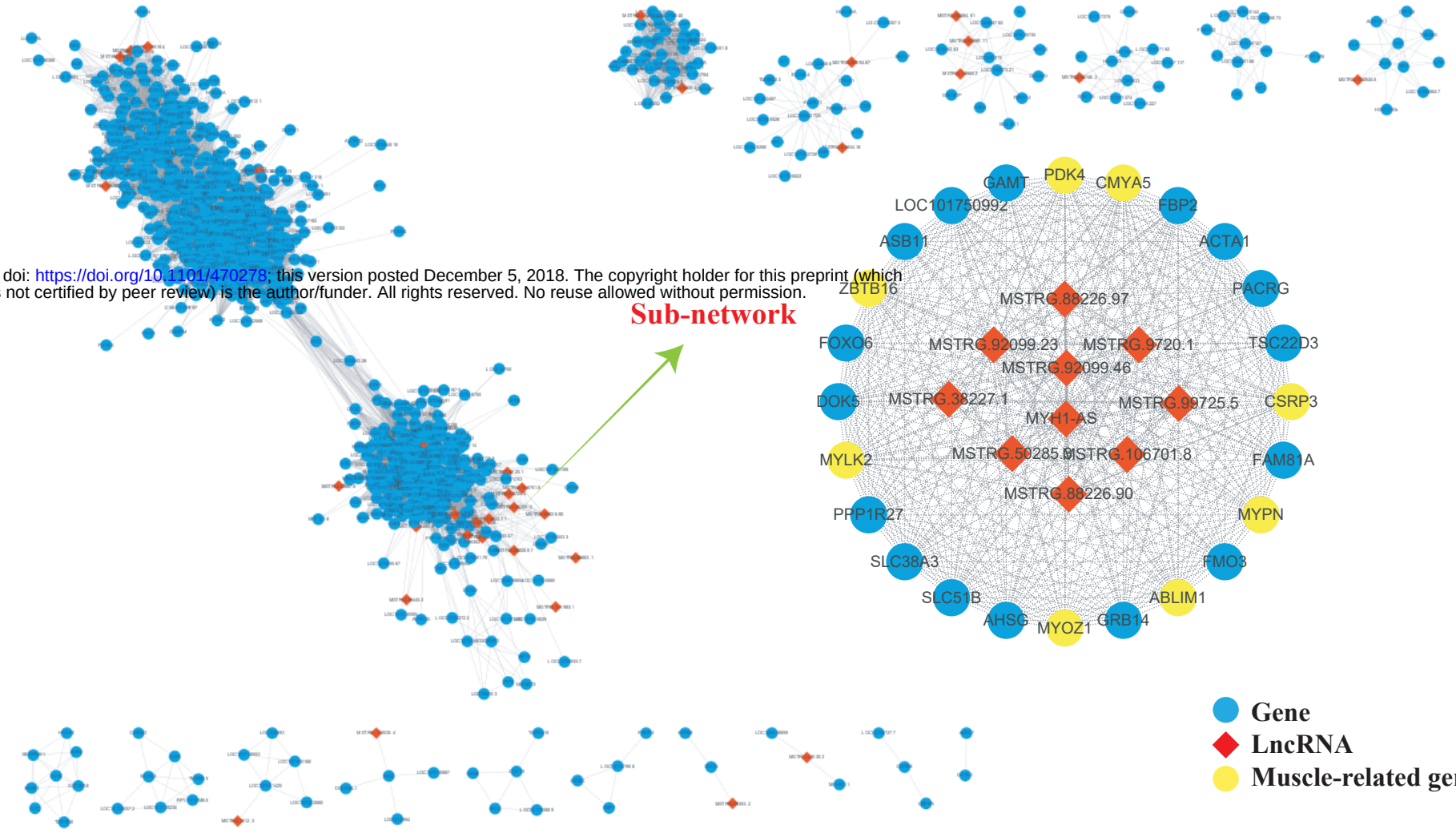

Fig 7e

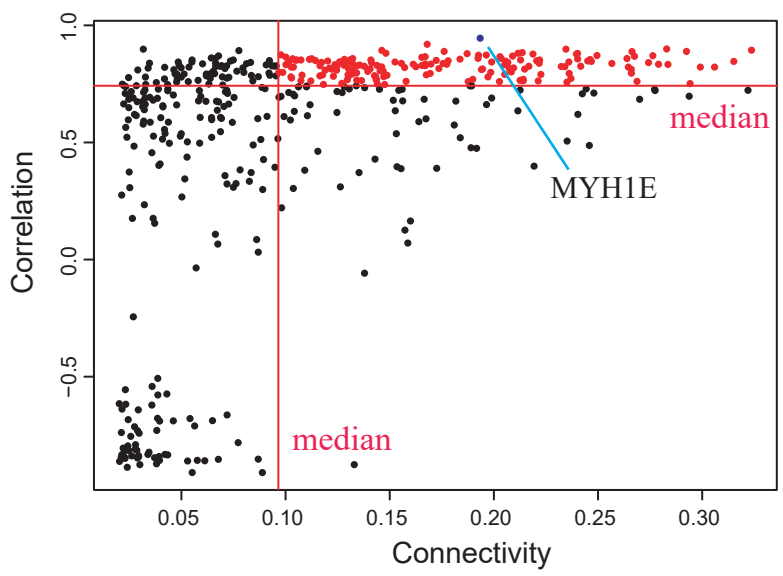

Fig 7f

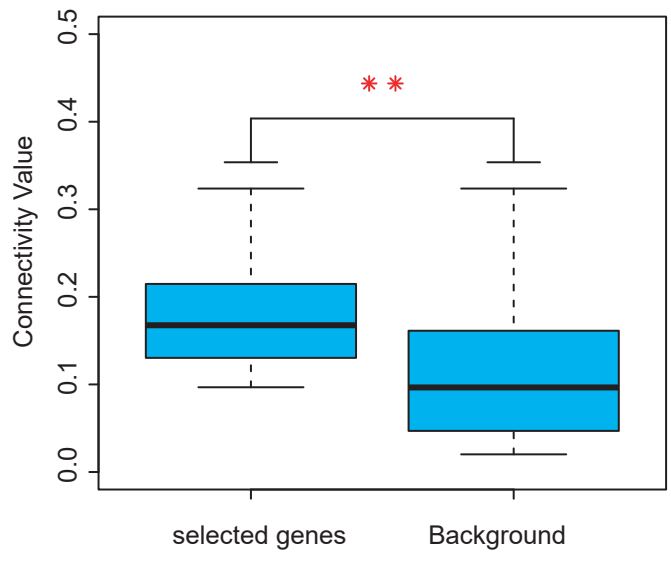

Fig 7g

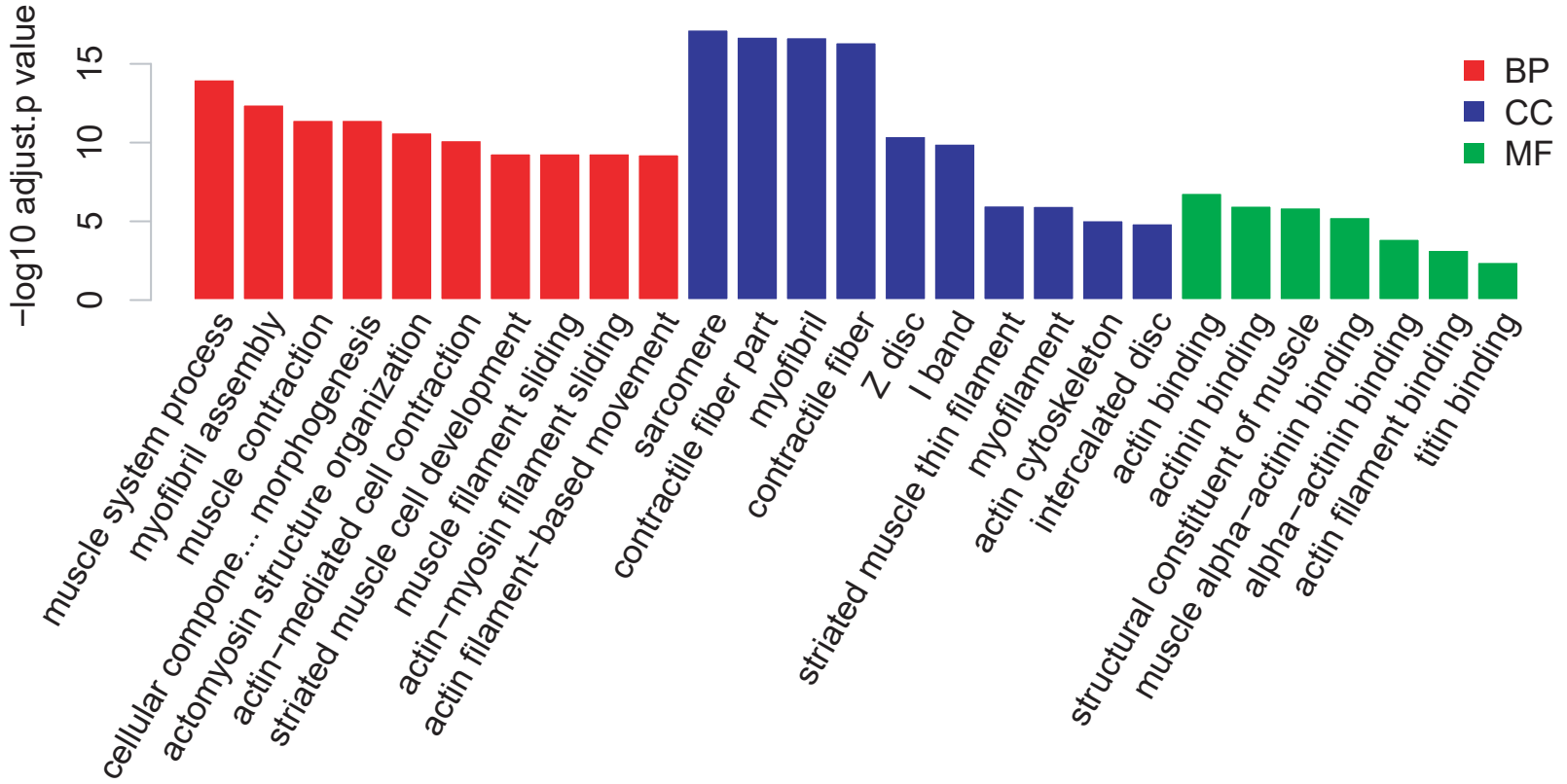

Fig 8a

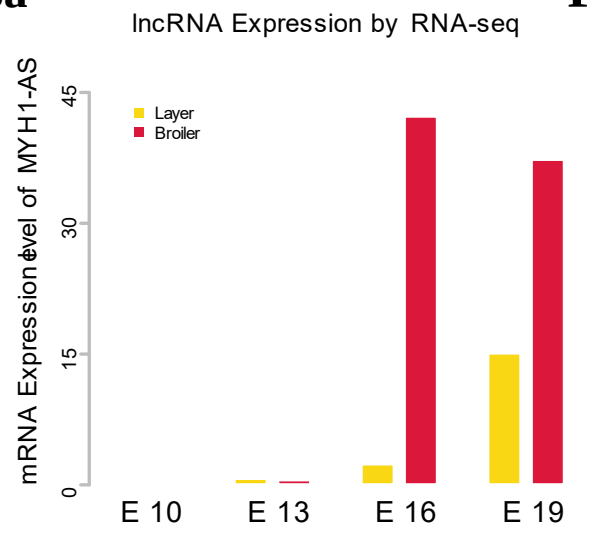

Fig 8b

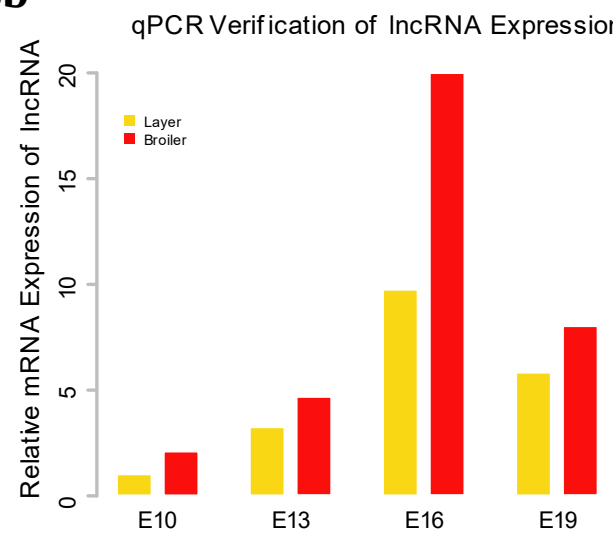

Fig 8c

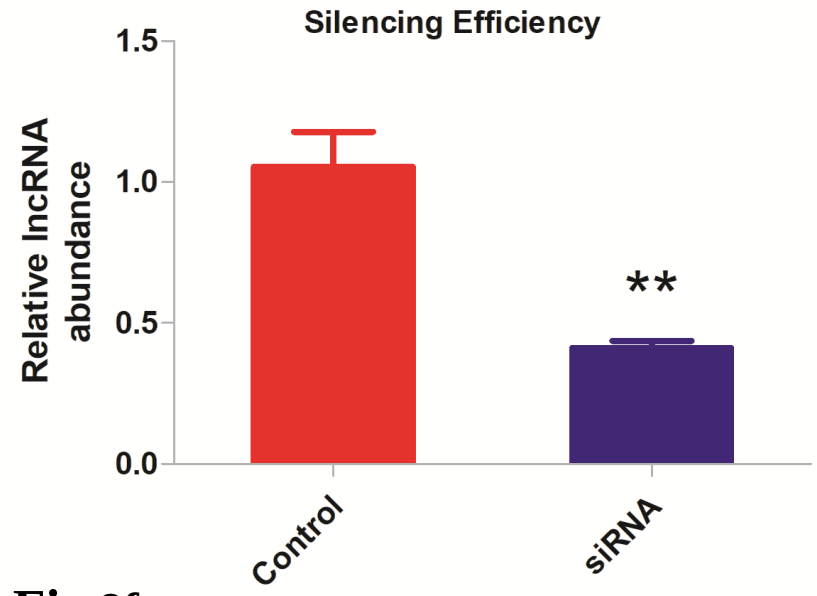

Fig 8d

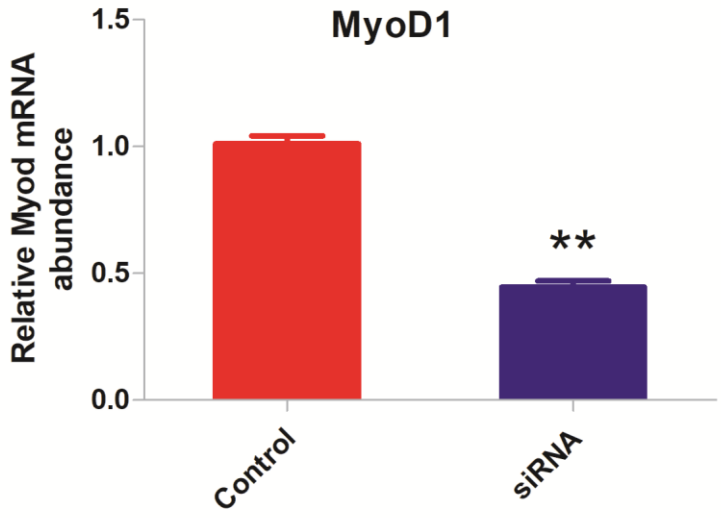

Fig 8e

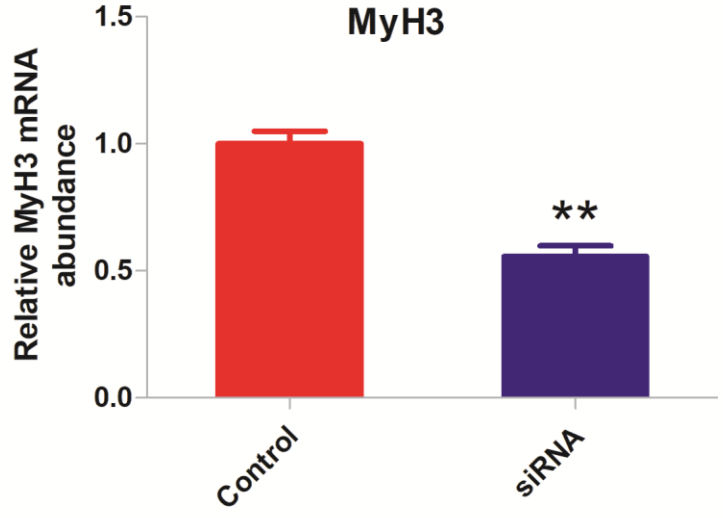

Fig 8f

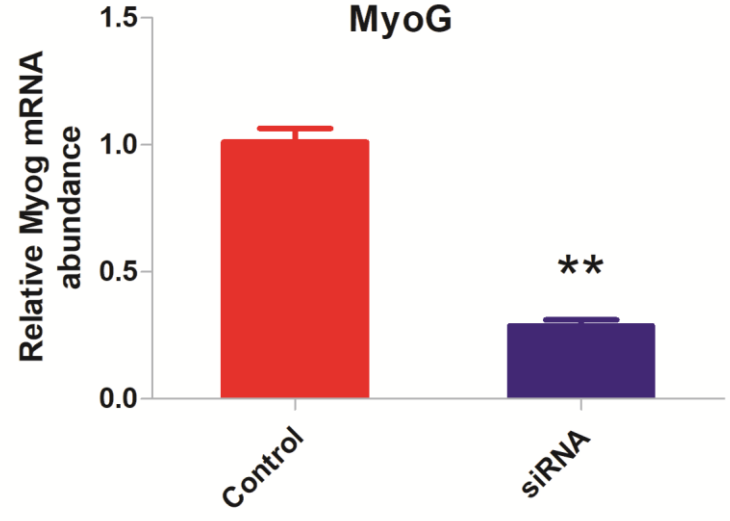

Fig 8g

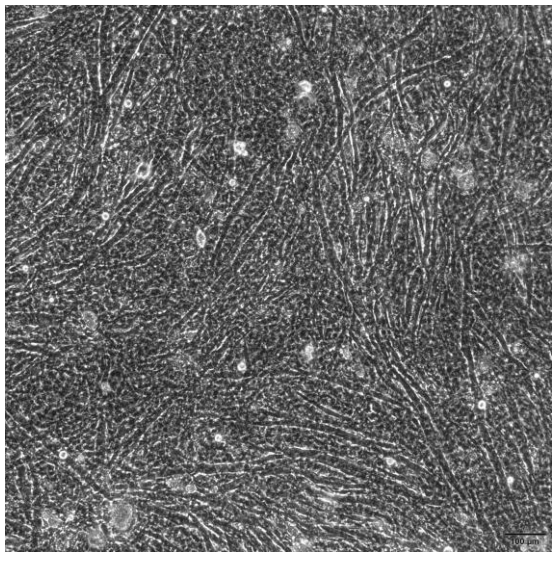

Fig 8h

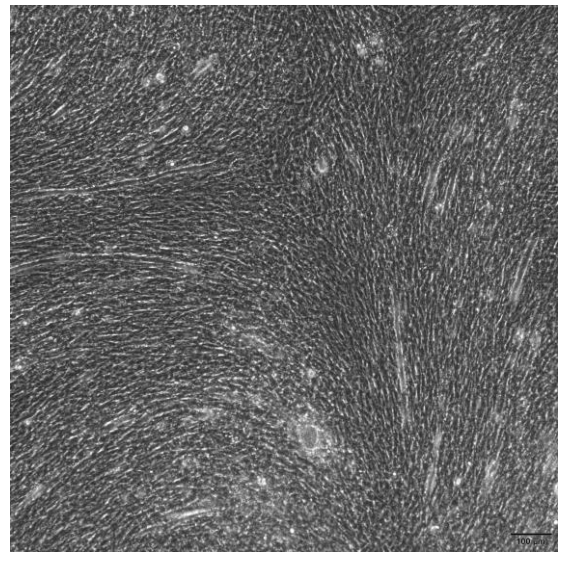

Fig 8i